Re-entrant corner flows of UCM fluids: The Cartesian stress basis

J.D. Evans*
Department of Mathematical Sciences, University of Bath,
Bath BA2 7AY, United Kingdom

April 28, 2006

Abstract

For a given re-entrant corner geometry, we describe a two parameter family of solutions for the local asymptotic behaviour of the flow and stress fields of UCM fluids. The two parameters used are the coefficients of the upstream wall shear rate and pressure gradient. In describing this parametric solution, the relationship between the Cartesian and natural stress basis is explained, reconciling these two equivalent formulations for the problem. The asymptotic solution structure investigated here comprises an outer (core) region together with inner regions (single wall boundary layers) located at the upstream and downstream walls. It is implicitly assumed that there are no regions of recirculation at the upstream wall i.e. we consider flow in the absence of a lip vortex. The essential features of the analysis is a full description of the matching between the outer and inner regions in both the Cartesian and natural stress bases, as well as the derivation of numerical estimates of important solution parameters such as the coefficients of the stream function and extra-stresses in the outer (core flow) region together with the downstream wall shear rate. This work is divided into two papers, this first one describing the solution structure in the Cartesian stress basis and the second using the natural stress basis.

Key words and phrases: UCM fluid; re-entrant corner; boundary layer; self-similar solutions; natural stress basis

* e-mail: masjde@maths.bath.ac.uk

1. Introduction

Substantial progress has been made recently on the local asymptotic analysis of the flow and stress fields associated with elastic fluids at re-entrant corners. The work of Rallinson and Hinch [7] used the natural stress basis formulation of Renardy [8] and [10], to analyze the boundary layer at the downstream wall for Oldroyd-B fluids. In contrast, Evans [1] and [3] used the Cartesian basis for the stress in the analysis of such a structure for UCM and Oldroyd-B fluids respectively. This recent work completes the analysis of the asymptotic regions previously known to comprise of a core flow classifying the stress singularity for such fluids as given by Hinch [6] and the upstream wall boundary layer analysis of Renardy [9]. It is natural to seek to understand how these approaches are linked in order to obtain a comprehensive understanding of the solution structure. This paper and its companion [5] will be concerned with the UCM model, extending the analytical and numerical analysis in Rallinson and Hinch [7] and Evans [1]. Implicit to the assumed solution structure is the absence of a lip vortex at the upstream wall. Comments on the case when such a feature is present are given in the discussion section.

The goals then are to:

1. reconcile the approaches of using Cartesian and natural stress bases,
2. describe the local asymptotic solution for flow and stress fields around a re-entrant corner of given angle as a two parameter family of solutions. The two parameters chosen are the coefficients of the upstream wall shear rate (or shear stress) and pressure gradient.

In addressing these goals, we will make extensive use of previous results. Many of the key mathematical results were determined in the seminal work of Hinch [6] and Renardy [8],[9],[10]. An important contribution of Rallinson and Hinch [7] was to show how these may be pieced together to give a full description for the problem as well as elucidating the presence of an essential singularity in the boundary layer equations at the downstream wall.

The work has been divided into a pair of papers, with this one concentrating on the Cartesian formulation of the problem and a companion paper [5] the natural stress basis. The layout of this paper is as follows. In the rest of this introduction we record the main mathematical results upon which the local asymptotic theory is constructed. The outer solution is addressed in section 2, whilst the boundary layer equations are analyzed in section 3. The new results in these sections are mainly concerned with the far-field behaviour of the stream function and stress components in both the upstream and downstream boundary layers. Consequently the full asymptotic expansion required in the core outer region can be determined as well as the corresponding behaviours for the natural stress variables. Additional new results concern the downstream wall behaviour where an essential singularity is known to exist (see Rallinson and Hinch [7]). The parametric solution description is then addressed in section 4 where the upstream and downstream boundary layers are considered separately. Numerical solution of the downstream layer is addressed, but we leave the determination of key parameters such as the downstream wall shear rate to the natural stress basis formulation in the companion paper.

For planar steady flow, the governing equations in dimensionless form are the momentum equation

$$\mathrm{Re}\,\mathbf{v}\cdot\nabla\mathbf{v} = -\nabla\,p + \nabla\cdot\mathbf{T} \tag{1.1}$$

the incompressibility condition

$$\nabla \cdot \mathbf{v} = 0 \tag{1.2}$$

and the constitutive relation

$$\mathbf{T} + \mathrm{We} \overset{\triangledown}{\mathbf{T}} = 2\mathbf{D}, \tag{1.3}$$

with the upper convected (or Oldroyd) stress derivative defined by

$$\overset{\triangledown}{\mathbf{T}} = (\mathbf{v} \cdot \nabla)\,\mathbf{T} - (\nabla \mathbf{v})\,\mathbf{T} - \mathbf{T}\,(\nabla \mathbf{v})^T$$

and

$$\mathbf{D} = \frac{1}{2} \nabla \mathbf{v} + (\nabla \mathbf{v})^T$$

being the rate-of-strain tensor. Here $\mathbf{T} = (T_{ij})$ is the extra-stress tensor, $\mathbf{v}$ is the velocity field, p is the pressure, Re is the Reynolds number and We is the Weissenberg number. The total stress tensor is given by $-p\mathbf{I} + \mathbf{T}$. These equations are taken to hold in the two dimensional sector $0 < r < \infty, 0 \leq \theta \leq \pi/\alpha$ with $\theta = 0$ representing the upstream wall and $\theta = \pi/\alpha$ the downstream wall ($1/2 \leq \alpha < 1$). Here, r is the radial distance from the corner and θ the polar angle. Our intention is to study the local asymptotics of the equations (1.1)–(1.3) as the corner is approached in the singular limit $r \to 0$. We now make the following preliminary remarks, before describing the detailed asymptotic structure of the solution.

Remark 1: Cartesian formulation. Initially Cartesian axes are taken with the x-axis along the upstream wall $\theta = 0$, and the y-axis along the ray $\theta = \pi/2$. Further, introducing the stream function ψ, the equations (1.1) and (1.3) can be written in the form

$$\mathrm{Re}\left(\frac{\partial \psi}{\partial y}\frac{\partial^2 \psi}{\partial x \partial y} - \frac{\partial \psi}{\partial x}\frac{\partial^2 \psi}{\partial y^2}\right) = -\frac{\partial p}{\partial x} + \frac{\partial T_{11}}{\partial x} + \frac{\partial T_{12}}{\partial y}, \tag{1.4}$$

$$\mathrm{Re}\left(-\frac{\partial \psi}{\partial y}\frac{\partial^2 \psi}{\partial x^2} + \frac{\partial \psi}{\partial x}\frac{\partial^2 \psi}{\partial y \partial x}\right) = -\frac{\partial p}{\partial y} + \frac{\partial T_{12}}{\partial x} + \frac{\partial T_{22}}{\partial y}, \tag{1.5}$$

and

$$T_{11} + \mathrm{We}\left(\frac{\partial \psi}{\partial y}\frac{\partial T_{11}}{\partial x} - \frac{\partial \psi}{\partial x}\frac{\partial T_{11}}{\partial y} - 2\frac{\partial^2 \psi}{\partial y^2}T_{12} - 2\frac{\partial^2 \psi}{\partial x \partial y}T_{11}\right) = 2\frac{\partial^2 \psi}{\partial x \partial y}, \tag{1.6}$$

$$T_{22} + \mathrm{We}\left(\frac{\partial \psi}{\partial y}\frac{\partial T_{22}}{\partial x} - \frac{\partial \psi}{\partial x}\frac{\partial T_{22}}{\partial y} + 2\frac{\partial^2 \psi}{\partial x^2}T_{12} + 2\frac{\partial^2 \psi}{\partial x \partial y}T_{22}\right) = -2\frac{\partial^2 \psi}{\partial x \partial y}, \tag{1.7}$$

$$T_{12} + \mathrm{We}\left(\frac{\partial \psi}{\partial y}\frac{\partial T_{12}}{\partial x} - \frac{\partial \psi}{\partial x}\frac{\partial T_{12}}{\partial y} + \frac{\partial^2 \psi}{\partial x^2}T_{11} - \frac{\partial^2 \psi}{\partial y^2}T_{22}\right) = \frac{\partial^2 \psi}{\partial y^2} - \frac{\partial^2 \psi}{\partial x^2}. \tag{1.8}$$

The indices $_1$ and $_2$ are associated with the x and y directions respectively, so that as usual

$$\mathbf{v} = (u, v) = \left(\frac{\partial \psi}{\partial y}, -\frac{\partial \psi}{\partial x}\right). \tag{1.9}$$

Remark 2: Weissenberg number set to unity. The problem has no natural length scale and thus the Weissenberg number may be removed from the formulation. The scalings that achieve this are

$$r \mapsto \frac{r}{\mathrm{We}^q}, \qquad \psi \mapsto \frac{\psi}{\mathrm{We}^{(2q-1)}}, \qquad \mathbf{T} \mapsto \mathrm{We}\mathbf{T}, \qquad p \mapsto \mathrm{We}p, \tag{1.10}$$

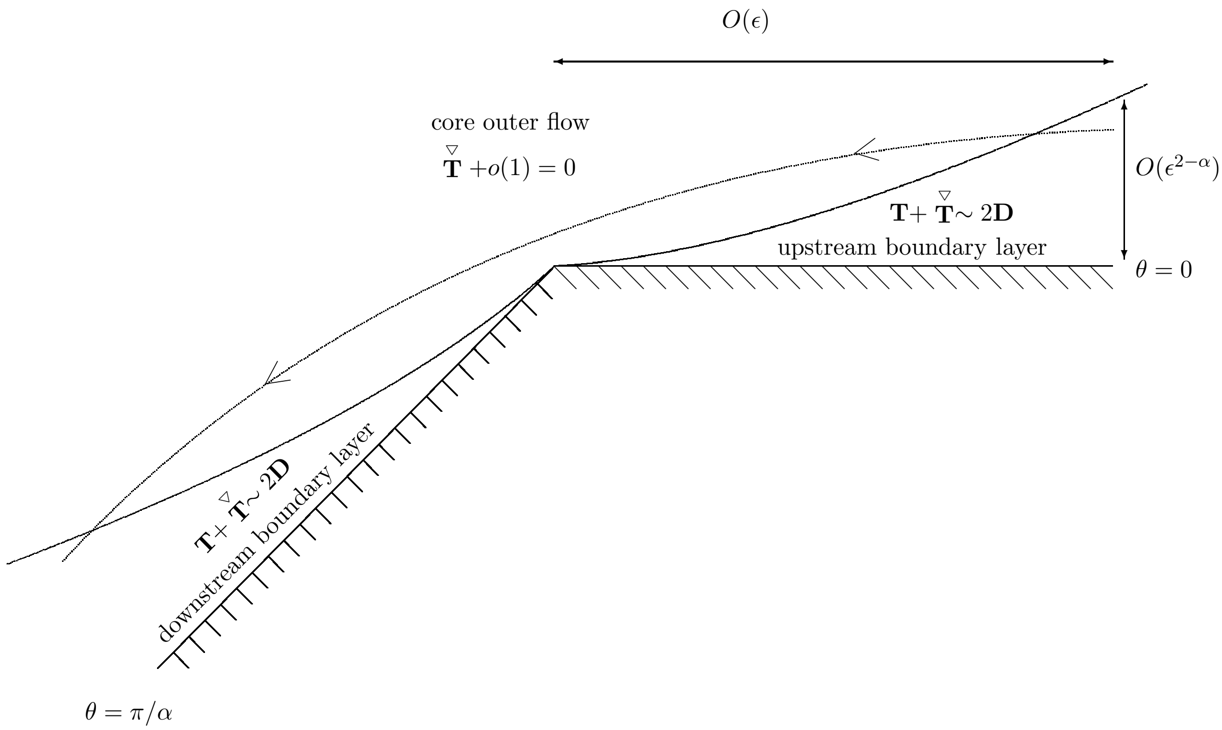

Figure 1: Schematic illustration of the asymptotic regions local to the re-entrant corner. Shown is a three region structure, comprising the outer or core flow region away from the boundaries and inner or boundary layers at the upstream and downstream walls. The fact that we are close to the corner is emphasized by showing that we are considering length scales of $O(\epsilon)$ from the corner where $\epsilon \ll 1$ is artificial parameter, introduced to aid determination of the sizes of terms in the governing equations in the respective regions. Shown is the upstream boundary layer being of thickness $O(\epsilon^{2-\alpha})$ on these length scales. A similar boundary layer structure is repeated at the downstream wall.

with the unique value $q = 1/2$ if the inertia terms are to be retained or any q when $\mathrm{Re} = 0$ and creeping flow is considered. It is also worth noting that under these scalings the inertia terms are negligible at leading order when $\mathrm{ReWe}^{(2q-1)} \ll 1$. Consequently we will take $\mathrm{We} = 1$ from now on. It is worth noting that these scalings break down in the limits $\mathrm{We} \to 0^+$ and $\mathrm{We} \to +\infty$, the resulting asymptotic structures being described in [2].

Remark 3: Wall boundary layers.

When considering the wall boundary layers, we will assume symmetry with respect to the upstream and downstream structures. Thus it will be sufficient to consider one structure only and for definiteness we take Cartesian axes aligned with the upstream wall. The downstream layer can then be considered by allowing for a change in the flow direction and re-orientation of the axes by the transformation

$$\psi \mapsto -\psi, \qquad y \mapsto -y, \qquad T_{12} \mapsto -T_{12}, \tag{1.11}$$

the other variables being unchanged. This transformation leaves the governing equations invariant and relative to the upstream layer, its net effect in the Cartesian formulation is to simply change the sign of the stream function when considering the downstream layer.

Remark 4: The leading order outer solution. In the outer (core) region, the fluid is assumed to advect and deform affinely, with the rate-of-strain and relaxation terms negligible in the constitutive equations. Consequently, the upper convected stress derivative terms dominate at leading order in (1.3), giving

$$(\mathbf{v}\cdot\nabla)\,\mathbf{T} - (\nabla\mathbf{v})\,\mathbf{T} - \mathbf{T}\,(\nabla\mathbf{v})^T = 0 \qquad \text{as } r\to 0. \tag{1.12}$$

Together with the momentum equation (1.1), this system has a relevant exact solution (first described by Hinch [6], with an alternative derivation given by Renardy [9]), namely

$$\psi = c_0 r^{\alpha n}\sin^n(\alpha\theta), \quad \mathbf{T} = \lambda\,(\psi)\,\mathbf{v}\mathbf{v}^T \qquad \text{as } r\to 0, \tag{1.13}$$

with

$$\lambda(\psi) = c_1\left(\frac{\psi}{c_0\alpha^n}\right)^{\frac{2}{n}-2},$$

where c_0, c_1 are arbitrary constants and the index n is to be determined. This class of self-similar solutions for the flow and stress fields gives

$$\psi = O(r^{n\alpha}), \quad \mathbf{T} = O(r^{-2(1-\alpha)}) \qquad \text{as } r\to 0$$

holding in the core outer region away from the walls. The stress singularity is determined and independent of the index n, which itself follows from matching of this outer solution to the wall boundary layers. For the single layer wall structures depicted in Figure 1, matching (see [1]) gives

$$n = 3-\alpha. \tag{1.14}$$

Other possible local flow structures are possible at a re-entrant corner in which reverse flow occurs at the upstream wall (see Evans [4]) and for which the index n lies in the interval $(3-\alpha, 2/\alpha)$ for $1/2 \le \alpha < 1$. However, such behaviours are not the focus of this current work and n will be assumed fixed and given by (1.14).

Remark 5: The approximation of $\mathbf{T}+\mathbf{I}$ by a rank one tensor. Renardy [11] noted that the extra-stress tensor satisfies the relationship

$$(\mathbf{v}.\nabla)(\det(\mathbf{T}+\mathbf{I})) = -\det(\mathbf{T}+\mathbf{I})\operatorname{tr}\left((\mathbf{T}+\mathbf{I})^{-1}\mathbf{T}\right).$$

This may be equivalently expressed as

$$(\mathbf{v}.\nabla)(\det(\mathbf{T}+\mathbf{I})) = -\det(\mathbf{T}+\mathbf{I})\left(2-\frac{\operatorname{tr}(\mathbf{T}+\mathbf{I})}{\det(\mathbf{T}+\mathbf{I})}\right), \tag{1.15}$$

where we note that

$$\det(\mathbf{T}+\mathbf{I}) = \lambda\nu - \mu^2. \tag{1.16}$$

The arguments used by Renardy in the high Weissenberg limit to deduce that the governing equations satisfy a form of the compressible Euler equations also applies to the We $= O(1)$ equations in the core outer region of re-entrant corners since in both cases the balance given by

(1.12) holds at leading order. For such regions then, $\mathbf{T}+\mathbf{I}$ is a rank one tensor at leading order and moreover we will show that

$$\det(\mathbf{T}+\mathbf{I}) = \Delta_0 \left(\frac{\psi}{c_0\alpha^n}\right)^{-\frac{2(1-\alpha)}{n}} \tag{1.17}$$

holds again at leading order in the core outer region. The constant Δ_0 will be determined by matching to the upstream boundary layer. This observation will be of particular use when considering the natural stress formulation.

2. The core flow outer solution

To make the sizes of terms in the governing equations clear and formulate a singular perturbation problem, it is convenient to introduce an artificial small parameter ϵ by the scalings

$$r = \epsilon R^*, \qquad x = \epsilon X^*, \qquad y = \epsilon Y^*, \tag{2.1}$$

where $0 < \epsilon \ll 1$, and consider first the region $R = O(1)$ away from the boundaries. Using the solution (1.13) we deduce the scalings for the extra-stresses, pressure and stream function as

$$\psi = \epsilon^{n\alpha}\Psi^*, \quad \mathbf{T} = \epsilon^{-2(1-\alpha)}\mathbf{T}^*, \quad p = \epsilon^{-2(1-\alpha)}p^*, \tag{2.2}$$

where we have retained the pressure gradient at leading order within the momentum equation. Consequently, the momentum and constitutive equations become

$$\mathrm{Re}\,\epsilon^{2(n-1)\alpha}\,\mathbf{v}^*\cdot\nabla^*\mathbf{v}^* = -\nabla^* p^* + \nabla^*\cdot\mathbf{T}^* \tag{2.3}$$

$$\epsilon^{2-n\alpha}\mathbf{T}^* + \overset{\triangledown}{\mathbf{T}}{}^* = \epsilon^{2(1-\alpha)}\left(\nabla^*\mathbf{v}^* + (\nabla^*\mathbf{v}^*)^T\right), \tag{2.4}$$

where we note that $\epsilon^{2-n\alpha} = \epsilon^{(2-\alpha)(1-\alpha)}$ when $n = 3-\alpha$.

Posing the expansions

$$\Psi^* = \Psi^{*(0)} + o(1), \quad \mathbf{T}^* = \mathbf{T}^{*(0)} + o(1), \quad p^* = p^{*(0)} + o(1), \qquad \text{as } \epsilon \to 0 \tag{2.5}$$

gives the leading order problem

$$0 = -\nabla^* p^{*(0)} + \nabla^*\cdot\mathbf{T}^{*(0)}, \qquad \overset{\triangledown}{\mathbf{T}}{}^{*(0)} = 0, \tag{2.6}$$

with solution

$$\Psi^{*(0)} = c_0 R^{*n\alpha}\sin^n(\alpha\theta), \tag{2.7}$$

which satisfies $\Psi^{*(0)} = 0$ on $\theta = 0$ and $\theta = \pi/\alpha$, and

$$T_{11}^{*(0)} = c_1\left(\frac{\Psi^{*(0)}}{c_0\alpha^n}\right)^{\frac{2}{n}-2}\left(\frac{\partial\Psi^{*(0)}}{\partial Y^*}\right)^2, \quad T_{12}^{*(0)} = -c_1\left(\frac{\Psi^{*(0)}}{c_0\alpha^n}\right)^{\frac{2}{n}-2}\left(\frac{\partial\Psi^{*(0)}}{\partial X^*}\frac{\partial\Psi^{*(0)}}{\partial Y^*}\right),$$

$$T_{22}^{*(0)} = c_1\left(\frac{\Psi^{*(0)}}{c_0\alpha^n}\right)^{\frac{2}{n}-2}\left(\frac{\partial\Psi^{*(0)}}{\partial X^*}\right)^2. \tag{2.8}$$

For matching with the boundary layers, we note the behaviour

$$\text{as } Y^* \to 0, \qquad \Psi^{*(0)} \sim C_0 X^{*(\alpha-1)n} Y^{*n}, \;\; p^{*(0)} \sim p_0 X^{*2(\alpha-1)}, \;\; T_{11}^{*(0)} \sim C_1 X^{*2(\alpha-1)},$$
$$T_{12}^{*(0)} \sim C_1(1-\alpha) X^{*(2\alpha-3)} Y^*, \;\; T_{22}^{*(0)} \sim C_1 (1-\alpha)^2 X^{*(2\alpha-4)} Y^{*2}. \tag{2.9}$$

where the following constants

$$C_0 = c_0 \alpha^n, \qquad C_1 = c_1 n^2 C_0^2, \qquad p_0 = \frac{1}{2} C_1, \tag{2.10}$$

are introduced for convenience.

The leading order matching conditions (2.9) when used with the appropriate dominant balance in the boundary layer, are sufficient to determine the boundary layer scalings and determine the index value $n = 3-\alpha$ (see [1]). However, as we shall see below, further terms in the expansion (2.5) are required if the downstream boundary layer equations are to be correctly specified. In fact, we shall see that we need to consider an expansion of the form

$$\begin{aligned}(\Psi^*, \mathbf{T}^*, p^*) = {} & (\Psi^{*(0)}, \mathbf{T}^{*(0)}, p^{*(0)}) + \epsilon^{2(1-\alpha)^2}(\Psi^{*(1)}, \mathbf{T}^{*(1)}, p^{*(1)}) + \epsilon^{(1-\alpha)}(\Psi^{*(2)}, \mathbf{T}^{*(2)}, p^{*(2)}) \\ & + \epsilon^{(2-\alpha)(1-\alpha)}(\Psi^{*(3)}, \mathbf{T}^{*(3)}, p^{*(3)}) + \epsilon^{2(1-\alpha)}(\Psi^{*(4)}, \mathbf{T}^{*(4)}, p^{*(4)}) + \epsilon^{(3-\alpha)(1-\alpha)}(\Psi^{*(5)}, \mathbf{T}^{*(5)}, p^{*(5)}) \\ & + \epsilon^{2(2-\alpha)(1-\alpha)}(\Psi^{*(6)}, \mathbf{T}^{*(6)}, p^{*(6)}) + \dots \\ & + \left[\epsilon^{4(1-\alpha)^2}(\hat{\Psi}^{*(2)}, \hat{\mathbf{T}}^{*(2)}, \hat{p}^{*(2)}) + \epsilon^{6(1-\alpha)^2}(\hat{\Psi}^{*(3)}, \hat{\mathbf{T}}^{*(3)}, \hat{p}^{*(3)}) + \dots\right] \quad \text{as } \epsilon \to 0. \end{aligned} \tag{2.11}$$

There are several points to be made about this expansion:

1. It is not uniform in $\alpha \in [1/2, 1)$. Specifically, the terms $O(\epsilon^{4(1-\alpha)^2})$ and $O(\epsilon^{6(1-\alpha)^2})$ change their relative ordering with the other terms in the expansion depending upon the value of α. Here we have extracted such terms from the main series and placed them in the square brackets. The expansion as given holds for $1/2 \leq \alpha \leq 2/3$ with the $O(\epsilon^{4(1-\alpha)^2})$ term intruding between the $O(\epsilon^{(2-\alpha)(1-\alpha)})$ and $O(\epsilon^{2(1-\alpha)})$ terms and similarly the $O(\epsilon^{6(1-\alpha)^2})$ term intruding between the $O(\epsilon^{2(1-\alpha)})$ and $O(\epsilon^{(3-\alpha)(1-\alpha)})$ terms. (At $\alpha = 2/3$ there is some redundancy in this expansion where terms can be combined.)

2. For $\alpha > 2/3$ then higher order terms in the square brackets need to be included e.g. of the form $O(\epsilon^{8(1-\alpha)^2})$. In fact, as $\alpha \to 1^-$, an ever increasing number of such terms need to be included. For $\alpha > 3/4$ it is worth noting that the $O(\epsilon^{4(1-\alpha)^2})$ term is now larger than the $O(\epsilon^{(1-\alpha)})$ term.

3. Terms of $O(\epsilon^{2(2-\alpha)(1-\alpha)})$ are the smallest terms that need to be considered, these being the last to contribute information to the leading order boundary layer equations.

4. Even to the orders recorded explicitly in this expansion, the inertia terms in the momentum equation are still subdominant and can be ignored if $\mathrm{Re} \leq O(1)$.

5. In principle we can pose the problems for each of the terms of the expansion. However, as we shall see, this is not necessary if we use the natural stress basis which will provide all the necessary information to the orders required. In fact, the main advantage of the natural stress basis is its ability to unpick the above expansion by extracting the leading order, $O(\epsilon^{(2-\alpha)(1-\alpha)})$ and $O(\epsilon^{2(2-\alpha)(1-\alpha)})$ terms. Such terms maintain their relative ordering with respect to each other uniformly in α.

It is worth recording that in the outer variables the expression (1.15) becomes

$$(\mathbf{v}^*.\nabla^*)(\det(\mathbf{T}^*+\epsilon^{2(1-\alpha)}\mathbf{I})) = -\epsilon^{(2-\alpha)(1-\alpha)}\det(\mathbf{T}^*+\epsilon^{2(1-\alpha)}\mathbf{I})\left(2-\epsilon^{2(1-\alpha)}\frac{\mathrm{tr}(\mathbf{T}^*+\epsilon^{2(1-\alpha)}\mathbf{I})}{\det(\mathbf{T}^*+\epsilon^{2(1-\alpha)}\mathbf{I})}\right).$$

We thus have that $\det(\mathbf{T}^*+\epsilon^{2(1-\alpha)}\mathbf{I})$ is constant along leading order streamlines. Assuming its behaviour to be an algebraic power of Ψ_0^* we thus have

$$\det(\mathbf{T}^*+\epsilon^{2(1-\alpha)}\mathbf{I}) = \epsilon^{m_1}\Delta_0\left(\frac{\Psi_0^*}{C_0}\right)^{m_2} \tag{2.12}$$

for some constant Δ_0 and powers m_1, m_2 which will be determined by matching to the upstream boundary layer.

Irrespective of the intricacies of the outer expansion, the neglect at leading order of the relaxation and rate-of-strain terms in (2.4) leads to the consideration of inner regions (boundary layers) located at the walls where the influence of such terms are important.

3. General boundary layer analysis

The stream function (2.7) and extra-stresses (2.8) do not give viscometric flow behaviour near the walls, where an inner solution is now sought. The boundary layer analysis that follows is performed in the axes orientation specified in the introduction and as such, it is directly applicable to the upstream wall. The same equations hold for the downstream boundary layer, allowing for a suitable re-orientation of the axes achieved through a scaling of variables as mentioned in Remark 3 in the introduction. At first we proceed generally before discussing separately the upstream and downstream situations.

Introducing $x=\epsilon\bar{X}$, dominant balance is given in (1.4)-(1.8) by the scalings

$$\begin{gathered} x=\epsilon\bar{X}, \quad y=\epsilon^{2-\alpha}\bar{Y}, \quad \psi=\epsilon^{3-\alpha}\bar{\Psi}, \\ p=\epsilon^{-2(1-\alpha)}\bar{p}, \quad T_{11}=\epsilon^{-2(1-\alpha)}\bar{T}_{11}, \quad T_{12}=\epsilon^{-(1-\alpha)}\bar{T}_{12}, \quad T_{22}=\bar{T}_{22}, \end{gathered} \tag{3.1}$$

or relating the outer and inner variables directly,

$$\begin{gathered} X^*=\bar{X}, \quad Y^*=\epsilon^{1-\alpha}\bar{Y}, \quad \Psi^*=\epsilon^{n(1-\alpha)}\bar{\Psi}, \\ p^*=\bar{p}, \quad T_{11}^*=\bar{T}_{11}, \quad T_{12}^*=\epsilon^{(1-\alpha)}\bar{T}_{12}, \quad T_{22}^*=\epsilon^{2(1-\alpha)}\bar{T}_{22}, \end{gathered} \tag{3.2}$$

on using (2.1) and (2.2). In $\bar{X}=O(1), \bar{Y}=O(1)$ we have the leading order equations

$$0=-\frac{d\bar{p}}{d\bar{X}}+\frac{\partial\bar{T}_{11}}{\partial\bar{X}}+\frac{\partial\bar{T}_{12}}{\partial\bar{Y}}, \tag{3.3}$$

$$\bar{T}_{11}+\left(\frac{\partial\bar{\Psi}}{\partial\bar{Y}}\frac{\partial\bar{T}_{11}}{\partial\bar{X}}-\frac{\partial\bar{\Psi}}{\partial\bar{X}}\frac{\partial\bar{T}_{11}}{\partial\bar{Y}}-2\frac{\partial^2\bar{\Psi}}{\partial\bar{Y}^2}\bar{T}_{12}-2\frac{\partial^2\bar{\Psi}}{\partial\bar{X}\partial\bar{Y}}\bar{T}_{11}\right)=0, \tag{3.4}$$

$$\bar{T}_{22}+\left(\frac{\partial\bar{\Psi}}{\partial\bar{Y}}\frac{\partial\bar{T}_{22}}{\partial\bar{X}}-\frac{\partial\bar{\Psi}}{\partial\bar{X}}\frac{\partial\bar{T}_{22}}{\partial\bar{Y}}+2\frac{\partial^2\bar{\Psi}}{\partial\bar{X}^2}\bar{T}_{12}+2\frac{\partial^2\bar{\Psi}}{\partial\bar{X}\partial\bar{Y}}\bar{T}_{22}\right)=-2\frac{\partial^2\bar{\Psi}}{\partial\bar{X}\partial\bar{Y}}, \tag{3.5}$$

$$\bar{T}_{12}+\left(\frac{\partial\bar{\Psi}}{\partial\bar{Y}}\frac{\partial\bar{T}_{12}}{\partial\bar{X}}-\frac{\partial\bar{\Psi}}{\partial\bar{X}}\frac{\partial\bar{T}_{12}}{\partial\bar{Y}}+\frac{\partial^2\bar{\Psi}}{\partial\bar{X}^2}\bar{T}_{11}-\frac{\partial^2\bar{\Psi}}{\partial\bar{Y}^2}\bar{T}_{22}\right)=\frac{\partial^2\bar{\Psi}}{\partial\bar{Y}^2}, \tag{3.6}$$

where $\bar{p} = \bar{p}(\bar{X})$ only, together with the wall conditions

$$\text{on} \quad \bar{Y} = 0, \quad \bar{\Psi} = \frac{\partial \bar{\Psi}}{\partial \bar{Y}} = 0, \tag{3.7}$$

and the matching conditions

$$\begin{aligned} \text{as } \bar{Y} \to \infty, \qquad \bar{\Psi} \sim C_0 \bar{X}^{(\alpha-1)n} \bar{Y}^n, \quad \bar{T}_{11} \sim C_1 \bar{X}^{2(\alpha-1)}, \\ \bar{T}_{12} = C_1(1-\alpha)\bar{X}^{(2\alpha-3)}\bar{Y}, \quad \bar{T}_{22} \sim C_1(1-\alpha)^2 \bar{X}^{(2\alpha-4)}\bar{Y}^2. \end{aligned} \tag{3.8}$$

These equations admit the similarity solution

$$\begin{aligned} \xi = \frac{\bar{Y}}{\bar{X}^{2-\alpha}}, \qquad \bar{\Psi} = \bar{X}^{3-\alpha} f(\xi), \qquad \bar{p} = p_0 \bar{X}^{2(\alpha-1)}, \\ \bar{T}_{11} = \bar{X}^{2(\alpha-1)} t_{11}(\xi), \qquad \bar{T}_{12} = \bar{X}^{(\alpha-1)} t_{12}(\xi), \qquad \bar{T}_{22} = t_{22}(\xi), \end{aligned} \tag{3.9}$$

to give

$$0 = 2(\alpha-1)(t_{11} - p_0) - (2-\alpha)\xi t_{11}' + t_{12}', \tag{3.10}$$

$$t_{11} + \big((\alpha-3) f t_{11}' + 2(\alpha-2)(f' - \xi f'') t_{11} - 2 f'' t_{12}\big) = 0, \tag{3.11}$$

$$\begin{aligned} t_{22} + \big((\alpha-3) f t_{22}' + 2(2-\alpha) \left((3-\alpha)(f - \xi f') + (2-\alpha)\xi^2 f''\right) t_{12} \\ +2(t_{22}+1)\left(f' - (2-\alpha)\xi f''\right)\big) = 0, \end{aligned} \tag{3.12}$$

$$\begin{aligned} t_{12} + \big((\alpha-3) f t_{12}' + (\alpha-1) f' t_{12} + (2-\alpha) \left((3-\alpha)(f - \xi f') + (2-\alpha)\xi^2 f''\right) t_{11} \\ -(t_{22}+1) f''\big) = 0, \end{aligned} \tag{3.13}$$

$$\text{at } \xi = 0, \qquad f = f' = 0, \tag{3.14}$$

$$\text{as } \xi \to \infty, \quad f \sim C_0 \xi^{(3-\alpha)}, \quad t_{11} \sim C_1, \quad t_{12} \sim C_1(1-\alpha)\xi, \quad t_{22} \sim C_1(1-\alpha)^2\xi^2. \tag{3.15}$$

This fifth-order system of equations with the specified boundary conditions possesses singularities of first kind (or a regular singularity) at $\xi = +\infty$ and second kind (or an irregular singularity) at $\xi = 0$. Consequently we now perform a local analysis around each of these singular points separately to determine the relevant asymptotic behaviours.

3.1 Viscometric behaviour at the wall

A local analysis at $\xi = 0$, for viscometric behaviour, shows that

$$\begin{aligned} f(\xi) &= \frac{1}{2} a \xi^2 + \frac{1}{3!} b \xi^3 + \frac{1}{4!} 3(1-\alpha)^2 a^3 \xi^4 + O(\xi^5), \\ t_{11}(\xi) &= 2a^2 + 2a(3(1-\alpha)a^2 + 2b)\xi + (12(3-2\alpha)(1-\alpha)a^4 + 6(4-3\alpha)a^2 b + 2b^2)\xi^2 + O(\xi^3), \\ t_{12}(\xi) &= a + (3(1-\alpha)a^2 + b)\xi + (4-3\alpha)(3(1-\alpha)a^2 + 2b)a\xi^2 + O(\xi^3), \\ t_{22}(\xi) &= 2(1-\alpha)a\xi + ((5-4\alpha)(1-\alpha)a^2 + (3-2\alpha)b)\xi^2 + O(\xi^3), \end{aligned} \tag{3.16}$$

where

$$a = f''(0), \qquad b = f'''(0), \tag{3.17}$$

are two free constants and

$$p_0 = \frac{1}{2}a^2 + \frac{1}{2(\alpha-1)}b. \tag{3.18}$$

The number of degrees of freedom contained in this asymptotic behaviour may be determined through an eigenmode analysis. We consider a perturbation of the form

$$\left(f(\xi), t_{ij}(\xi)\right) \sim \left(f^{(0)}(\xi), t_{ij}^{(0)}(\xi)\right) + \hat{\delta}\left(\hat{f}(\xi), \hat{t}_{ij}(\xi)\right), \qquad \text{as } \xi \to 0 \tag{3.19}$$

where $i, j \in \{1, 2\}$, $f^{(0)}(\xi)$ and $t_{ij}^{(0)}(\xi)$ represent the regular power series expansion terms (the first few terms being recorded in (3.16)) and $\hat{\delta}$ is a small artificial gauge. Keeping terms of $O(\hat{\delta})$, the linearized equations satisfied by $\hat{f}(\xi), \hat{t}_{ij}(\xi)$ are

$$\begin{aligned}
&0 = 2(\alpha-1)\hat{t}_{11} - (2-\alpha)\xi\hat{t}_{11}' + \hat{t}_{12}', \\
&\hat{t}_{11} + (\alpha-3)\left(f^{(0)}\hat{t}_{11}' + \hat{f}t_{11}^{(0)\prime}\right) + 2(\alpha-2)\left(f^{(0)\prime} - \xi f^{(0)\prime\prime}\right)\hat{t}_{11} \\
&\qquad +2(\alpha-2)\left(\hat{f}' - \xi\hat{f}''\right)t_{11}^{(0)} - 2f^{(0)\prime\prime}\hat{t}_{12} - 2\hat{f}''t_{12}^{(0)} = 0, \\
&\hat{t}_{22} + (\alpha-3)\left(f^{(0)}\hat{t}_{22}' + \hat{f}t_{22}^{(0)}\right) + 2(2-\alpha)\left((3-\alpha)(f^{(0)} - \xi f^{(0)\prime}) + (2-\alpha)\xi^2 f^{(0)\prime\prime}\right)\hat{t}_{12} \\
&\qquad +2(2-\alpha)\left((3-\alpha)(\hat{f} - \xi\hat{f}') + (2-\alpha)\xi^2\hat{f}''\right)t_{12}^{(0)} + 2(t_{22}^{(0)} + 1)\left(\hat{f}' - (2-\alpha)\xi\hat{f}''\right) \\
&\qquad +2\hat{t}_{22}\left(f^{(0)\prime} - (2-\alpha)\xi f^{(0)\prime\prime}\right) = 0, \\
&\hat{t}_{12} + (\alpha-3)\left(f^{(0)}\hat{t}_{12}' + \hat{f}t_{12}^{(0)\prime}\right) + (\alpha-1)\left(f^{(0)\prime}\hat{t}_{12} + \hat{f}'t_{12}^{(0)}\right) \\
&\qquad +(2-\alpha)\left((3-\alpha)(f^{(0)} - \xi f^{(0)\prime}) + (2-\alpha)\xi^2 f^{(0)\prime\prime}\right)\hat{t}_{11} \\
&\qquad +(2-\alpha)\left((3-\alpha)(\hat{f} - \xi\hat{f}') + (2-\alpha)\xi^2\hat{f}''\right)t_{11}^{(0)} - (t_{22}^{(0)} + 1)\hat{f}'' - \hat{t}_{22}^{(0)}f^{(0)\prime\prime} = 0,
\end{aligned}$$

which have the following five asymptotic behaviours as $\xi \to 0$,

$$\left.\begin{array}{c}
\hat{f} \sim 1 \\
\hat{t}_{11} \sim -2(3-\alpha)a(4\alpha a^2 - 3b) \\
\hat{t}_{12} \sim -(3-\alpha)((3+\alpha)a^2 - b) \\
\hat{t}_{22} \sim -2(3-\alpha)a
\end{array}\right\}; \quad
\left.\begin{array}{c}
\hat{f} \sim \xi \\
\hat{t}_{11} \sim 6(1-\alpha)a^2 \\
\hat{t}_{12} \sim -(1+\alpha)a \\
\hat{t}_{22} \sim -2
\end{array}\right\}; \quad
\left.\begin{array}{c}
\hat{f} \sim \xi^2 \\
\hat{t}_{11} \sim 8a \\
\hat{t}_{12} \sim 2 \\
\hat{t}_{22} \sim 4(1-\alpha)\xi
\end{array}\right\};$$

$$\left.\begin{array}{c}
\hat{f} \sim \xi^{q_1+5}\exp\left(-\frac{2}{a(3-\alpha)\xi}\right) \\
\hat{t}_{11} \sim -\frac{16}{3(3-\alpha)^3a^2}\xi^{q_1}\exp\left(-\frac{2}{a(3-\alpha)\xi}\right) \\
\hat{t}_{12} \sim -\frac{16(2-\alpha)}{3(3-\alpha)^3a^2}\xi^{q_1+1}\exp\left(-\frac{2}{a(3-\alpha)\xi}\right) \\
\hat{t}_{22} \sim -\frac{4}{(3-\alpha)^2a^3}\xi^{q_1+1}\exp\left(-\frac{2}{a(3-\alpha)\xi}\right)
\end{array}\right\}; \quad
\left.\begin{array}{c}
\hat{f} = o\left(\xi^{q_2+6}\exp\left(-\frac{2}{a(3-\alpha)\xi}\right)\right) \\
\hat{t}_{11} \sim \xi^{q_2}\exp\left(-\frac{2}{a(3-\alpha)\xi}\right) \\
\hat{t}_{12} \sim (2-\alpha)\xi^{q_2+1}\exp\left(-\frac{2}{a(3-\alpha)\xi}\right) \\
\hat{t}_{22} = (2-\alpha)^2\xi^{q_2+2}\exp\left(-\frac{2}{a(3-\alpha)\xi}\right)
\end{array}\right\}; \tag{3.20}$$

where

$$q_1 = \frac{(1+\alpha)}{(3-\alpha)} - \frac{2b}{3(3-\alpha)a^2}, \qquad q_2 = -4\frac{(2-\alpha)}{(3-\alpha)} - \frac{2b}{3(3-\alpha)a^2}. \tag{3.21}$$

The first two modes are always inconsistent with the asymptotic behaviour (3.16), whereas the third mode is always consistent and corresponds to small changes in the free constant a. The behaviour of the fourth and fifth modes depend crucially on the sign of a. They are exponentially large and inconsistent with the expansion (3.16) if $a < 0$ whereas they are both exponentially small and consistent if $a > 0$.

Consequently we can deduce the following:

1. In the case $a < 0$, all modes apart from the third are asymptotically inconsistent with the expansion (3.16) implying that it has only one degree of freedom, namely that associated with the constant a. The local expansion at the wall being analytic in this case.

2. In the case $a > 0$, only the first and second modes are asymptotically inconsistent with the expansion (3.16) implying that it has three degrees of freedom. There is one degree of freedom associated with the constant a and a further two associated with the exponentially small terms. In this case, the wall expansion as posed in (3.16) hides the fact that it is no longer necessarily analytic, with the presence of two sets of exponentially small terms i.e. we have the presence of an essential singularity with two degrees of freedom. The local expansion in this case takes the form

$$\begin{aligned}
f(\xi) &= \frac{1}{2}a\xi^2 + \frac{1}{3!}b\xi^3 + \frac{1}{4!}3(1-\alpha)^2a^3\xi^4 + \ldots + K_1\xi^{q_1+5}\exp\left(-\frac{2}{a(3-\alpha)\xi}\right)(1+O(\xi)),\\
t_{11}(\xi) &= 2a^2 + 2a(3(1-\alpha)a^2+2b)\xi + (12(3-2\alpha)(1-\alpha)a^4 + 6(4-3\alpha)a^2b + 2b^2)\xi^2 + \ldots\\
&\quad - \frac{16K_1}{3(3-\alpha)^3a^2}\xi^{q_1}\exp\left(-\frac{2}{a(3-\alpha)\xi}\right)(1+O(\xi)) + K_2\xi^{q_2}\exp\left(-\frac{2}{a(3-\alpha)\xi}\right)(1+O(\xi)),\\
t_{12}(\xi) &= a + (3(1-\alpha)a^2+b)\xi + (4-3\alpha)(3(1-\alpha)a^2+2b)a\xi^2 + \ldots\\
&\quad - \frac{16(2-\alpha)K_1}{3(3-\alpha)^3a^2}\xi^{q_1+1}\exp\left(-\frac{2}{a(3-\alpha)\xi}\right)(1+O(\xi)) + K_2(2-\alpha)\xi^{q_2+1}\exp\left(-\frac{2}{a(3-\alpha)\xi}\right)(1+O(\xi)),\\
t_{22}(\xi) &= 2(1-\alpha)a\xi + ((5-4\alpha)(1-\alpha)a^2 + (3-2\alpha)b)\xi^2 + \ldots\\
&\quad - \frac{4K_1}{(3-\alpha)^2a^3}\xi^{q_1+1}\exp\left(-\frac{2}{a(3-\alpha)\xi}\right)(1+O(\xi)) + K_2(2-\alpha)^2\xi^{q_2+2}\exp\left(-\frac{2}{a(3-\alpha)\xi}\right)(1+O(\xi)),
\end{aligned} \tag{3.22}$$

   where q_1, q_2 are as given in (3.21). The exponentially small terms can be obtained by using a standard WKBJ expansion for the hat variables in the asymptotic form (3.19) and thus are the same as the fourth and fifth eigenmodes. The three degrees of freedom are represented by the constants a, K_1, K_2. We note that this local wall expansion can be considered as being composed of an analytic part (the power series terms in regular powers of ξ) and non-analytic part involving two sets of exponentially small terms. The controlling factor for both sets of exponentially small terms is the same, whilst the powers q_1, q_2 are not integers in general.

3. The borderline case $a = 0$ is discussed in Appendix A. Now there are no degrees of freedom in the case $b < 0$, whilst there are two in the case $b > 0$, both associated with exponentially small terms. The case $b = 0$ gives $p_0 = 0$ and is not expected to yield non trivial solutions.

3.2 The far-field behaviour

The far-field behaviour (3.15) together with (3.10) implies that the constant p_0 satisfies

$$p_0 = \frac{1}{2}C_1. \tag{3.23}$$

In a similar manner to the wall behaviour, we can determine the number of degrees of freedom in the far-field behaviour. Writing

$$f \sim C_0\xi^{3-\alpha}(1+\hat{\delta}\hat{f}(\xi)), \quad t_{11} \sim C_1(1+\hat{\delta}\hat{t}_{11}(\xi)), \quad t_{12} \sim C_1(1-\alpha)\xi(1+\hat{\delta}\hat{t}_{12}(\xi)),$$
$$t_{22} \sim C_1(1-\alpha)^2\xi^2(1+\hat{\delta}\hat{t}_{22}(\xi)), \tag{3.24}$$

linearization about (3.15) gives the asymptotic behaviours for the eigenmodes as

$$\left.\begin{array}{l} \hat{f}=1 \\ \hat{t}_{11}=0 \\ \hat{t}_{12}=0 \\ \hat{t}_{22}=0 \end{array}\right\};\ \left.\begin{array}{l} \hat{f}=\xi^{-2+2\alpha} \\ \hat{t}_{11}=\frac{2(2\alpha-1)}{(3-\alpha)}\xi^{-2+2\alpha} \\ \hat{t}_{12}=-\frac{4(1-\alpha)}{(3-\alpha)}\xi^{-2+2\alpha} \\ \hat{t}_{22}=-\frac{2(3-2\alpha)}{(3-\alpha)}\xi^{-2+2\alpha} \end{array}\right\};\ \left.\begin{array}{l} \hat{f}=\xi^{-1} \\ \hat{t}_{11}=0 \\ \hat{t}_{12}=-\frac{1}{(1-\alpha)(3-\alpha)}\xi^{-1} \\ \hat{t}_{22}=-\frac{2}{(1-\alpha)(3-\alpha)}\xi^{-1} \end{array}\right\};$$

$$\left.\begin{array}{l} \hat{f}=\xi^{-2+\alpha} \\ \hat{t}_{11}=-\frac{2(1-\alpha)}{(1+\alpha)(3-\alpha)}\xi^{-2+\alpha} \\ \hat{t}_{12}=-\frac{2(\alpha^2-2\alpha+2)}{(1-\alpha^2)(3-\alpha)}\xi^{-2+\alpha} \\ \hat{t}_{22}=-\frac{2(\alpha^2-2\alpha+3)}{(1-\alpha^2)(3-\alpha)}\xi^{-2+\alpha} \end{array}\right\};\ \left.\begin{array}{l} \hat{f}=\xi^{-4+2\alpha} \\ \hat{t}_{11}=\frac{2(1-\alpha)(3-2\alpha)}{\alpha(3-\alpha)}\xi^{-4+2\alpha} \\ \hat{t}_{12}=\frac{4(3-3\alpha+\alpha^2)}{\alpha(3-\alpha)}\xi^{-4+2\alpha} \\ \hat{t}_{22}=\frac{2(3-3\alpha+\alpha^2)(4-5\alpha+2\alpha^2)}{\alpha(1-\alpha)^2(3-\alpha)}\xi^{-4+2\alpha} \end{array}\right\}. \tag{3.25}$$

As noted in [1], all modes are consistent with the behaviour (3.15) the implication being that it may be termed generic and contains five degrees of freedom. The correct specification of our problem requires that we obtain further terms in the far-field expansion. Proceeding systematically for the equations (3.10)–(3.13) by identifying and determining each successive term in the expansion (the eigenmodes being helpful in this respect for determining the homogeneous terms) we obtain the far-field expansion as

$$
\begin{aligned}
f(\xi) \sim C_0\xi^{3-\alpha}\Bigg(&1 + C_2\xi^{-2+2\alpha} + \Big[F_2 C_2^2\xi^{-4+4\alpha} - F_3 C_2^3\xi^{-6+6\alpha}\Big] \\
&+C_3\xi^{-1} + \left(\frac{1}{2(2-\alpha)C_0} + C_4\right)\xi^{-2+\alpha} + \frac{(2-\alpha)C_3^2}{2(3-\alpha)}\xi^{-2} + \frac{C_1(1+2(2-\alpha)C_0C_4)}{2(2-\alpha)(3-\alpha)C_0}\xi^{-3+\alpha} + C_5\xi^{-4+2\alpha}\Bigg),
\end{aligned}
\tag{3.26}
$$

$$
\begin{aligned}
t_{11}(\xi) \sim C_1\Bigg(&1 + \frac{2(2\alpha-1)C_2}{(3-\alpha)}\xi^{-2+2\alpha} + \Big[A_2C_2^2\xi^{-4+4\alpha} - A_3C_2^3\xi^{-6+6\alpha}\Big] \\
&-\frac{2(1-\alpha)C_4}{(1+\alpha)(3-\alpha)}\xi^{-2+\alpha} + \frac{2(1-\alpha)(2-\alpha)C_1C_4)}{(1+\alpha)(3-\alpha)^2}\xi^{-3+\alpha} \\
&+\frac{2(1-\alpha)(3-2\alpha)}{\alpha(3-\alpha)}\left(C_5 + \frac{C_4(3-\alpha+2(1-\alpha)(2-\alpha)C_0C_4)}{4(1+\alpha)(2-\alpha)(3-\alpha)C_0}\right)\xi^{-4+2\alpha}\Bigg),
\end{aligned}
\tag{3.27}
$$

$$
\begin{aligned}
t_{12}(\xi) \sim C_1(1-\alpha)\xi\Bigg(&1 - \frac{4(1-\alpha)C_2}{(3-\alpha)}\xi^{-2+2\alpha} + \Big[B_2C_2^2\xi^{-4+4\alpha} - B_3C_2^3\xi^{-6+6\alpha}\Big] \\
&-\frac{C_3}{(1-\alpha)(3-\alpha)}\xi^{-1} - \frac{2(\alpha^2-2\alpha+2)C_4}{(1-\alpha^2)(3-\alpha)}\xi^{-2+\alpha} + \frac{2(\alpha^2-3\alpha+4)C_1C_4)}{(1+\alpha)(3-\alpha)^2}\xi^{-3+\alpha} \\
&+\frac{4(3-3\alpha+\alpha^2)}{\alpha(3-\alpha)}\left(C_5 - \frac{(3-\alpha+2(1-\alpha)(2-\alpha)C_0C_4)C_4}{4(1+\alpha)(2-\alpha)(3-\alpha)}\right)\xi^{-4+2\alpha}\Bigg),
\end{aligned}
\tag{3.28}
$$

$$
\begin{aligned}
t_{22}(\xi) \sim C_1(1-\alpha)^2\xi^2\Bigg(&1 - \frac{2(3-2\alpha)C_2}{(3-\alpha)}\xi^{-2+2\alpha} + \Big[D_2C_2^2\xi^{-4+4\alpha} - D_3C_2^3\xi^{-6+6\alpha}\Big] \\
&-\frac{2C_3}{(1-\alpha)(3-\alpha)}\xi^{-1} - \frac{2(\alpha^2-2\alpha+3)C_4}{(1-\alpha^2)(3-\alpha)}\xi^{-2+\alpha} + \frac{(C_1^2C_3^2-(3-\alpha)^2)}{C_1(1-\alpha)^2(3-\alpha)^2}\xi^{-2} \\
&+\frac{2(\alpha^4-5\alpha^2+13\alpha^2-15\alpha+8)C_1C_4)}{(1+\alpha)(1-\alpha)^2(3-\alpha)^2}\xi^{-3+\alpha} + \Bigg(\frac{2C_5(3-3\alpha+\alpha^2)(4-5\alpha+2\alpha^2)}{\alpha(3-\alpha)(1-\alpha)^2} \\
&-\frac{(2\alpha^4-11\alpha^3+26\alpha^2-27\alpha+12)(3-\alpha+2(1-\alpha)(2-\alpha)C_0C_4)C_4}{2\alpha(1-\alpha)^2(1+\alpha)(2-\alpha)(3-\alpha)^2C_0}\Bigg)\xi^{-4+2\alpha}\Bigg),
\end{aligned}
\tag{3.29}
$$

where

$$
\begin{aligned}
F_2 &= \frac{3(1-\alpha)}{2(3-4\alpha)(3-\alpha)}, & F_3 &= \frac{(1-\alpha)(22\alpha^2-47\alpha+15)}{6(3-4\alpha)(5-6\alpha)(3-\alpha)^2}, \\
A_2 &= \frac{4(1-\alpha)(1-2\alpha)}{(3-\alpha)^2}, & A_3 &= \frac{(1-\alpha)(1-2\alpha)(2-3\alpha)(3-2\alpha)}{(3-4\alpha)(3-\alpha)^3}, \\
B_2 &= \frac{8(1-\alpha)(1-2\alpha)(3-2\alpha)}{(3-4\alpha)(3-\alpha)^2}, & B_3 &= \frac{8(1-\alpha)(1-2\alpha)(2-3\alpha)(3-2\alpha)(5-3\alpha)}{(3-4\alpha)(5-6\alpha)(3-\alpha)^3}, \\
D_2 &= \frac{4(3-2\alpha)(4\alpha^2-9\alpha+4)}{(3-4\alpha)(3-\alpha)^2}, & D_3 &= \frac{4(1-2\alpha)(3-2\alpha)(5-3\alpha)(6\alpha^2-15\alpha+8)}{(3-4\alpha)(5-6\alpha)(3-\alpha)^3}.
\end{aligned}
\tag{3.30}
$$

This expansion now contains the five free constants $(C_0, C_2, C_3, C_4, C_5)$, each eigenmode corresponding to small changes in one of these free constants. The constant C_1 is fixed and not free due to (3.23) and the implicit assumption used in our eigenmode analysis that p_0 is fixed. We now make several remarks on this expansion:

1. It is not uniform in α. The terms in square brackets are the higher order forced terms arising from the second eigenmode behaviour. These terms change their relative order with the other terms in the expansion as α varies. For this reason they have been grouped together.

2. The expansion as recorded is only valid for $1/2 \leq \alpha \leq 2/3$. For $2/3 < \alpha < 1$, additional terms arising from the forcing of the second eigenmode enter the expansion, for example, terms $O(\xi^{-8+8\alpha}), O(\xi^{-10+10\alpha})$ etc. are required to be added to the terms in the square brackets. As $\alpha \to 1^-$, an ever increasing number of such terms are required. Moreover the coefficients of such terms are singular at specific α values, for example, $\alpha = 3/4$ and $\alpha = 5/6$. It is reasonable to conjecture that there are sequence of such values accumulating at $\alpha = 1$. At these specific values the expansion needs minor modification with respect to the higher order terms involving the free constant C_2 (probably through the inclusion of logarithmic terms such as $\xi^{-4+4\alpha} \ln \xi$ in place of $\xi^{-4+4\alpha}$ for example).

3. The other terms in the expansion that are not enclosed in square brackets maintain their relative ordering uniformly in α.

We are now in a position to determine the unknown constants in (2.12). Writing (2.12) in inner similarity variables using (3.1) and (3.9) gives

$$\bar{X}^{2(\alpha-1)}\epsilon^{2(1-\alpha)}\Big((t_{11}(\xi)+\epsilon^{2(1-\alpha)})(t_{22}(\xi)+1)-t_{12}(\xi)^2\Big) = \bar{X}^{nm_2}\epsilon^{m_1+n(1-\alpha)m_2}\Delta_0 f(\xi)^{nm_2}$$

and thus

$$m_1 = 2(2-\alpha)(1-\alpha), \qquad m_2 = \frac{2(\alpha-1)}{n}, \tag{3.31}$$

on balancing the $\bar{X}$ and ϵ dependence. Using the far-field behaviour in (3.15) for $f(\xi)$, we thus obtain the behaviour

$$t_{11}(1+t_{22}) - t_{12}^2 \sim \Delta_0 \xi^{-2+2\alpha} \qquad \text{as } \xi \to \infty \tag{3.32}$$

for the leading order matching of $\det(\mathbf{T}+\mathbf{I})$ between the inner and outer regions. It may be verified that the expressions (3.27)–(3.29) satisfy (3.32) with the constant Δ_0 given by

$$\Delta_0 = \frac{2(3-2\alpha)}{\alpha(3-\alpha)}C_1^2C_5 - \frac{(\alpha^2-2\alpha+3)}{2\alpha(1+\alpha)(2-\alpha)(3-\alpha)}\frac{C_1^2C_4}{C_0} + \frac{(\alpha^4-2\alpha^3+2\alpha^2-2\alpha-3)}{\alpha(1+\alpha)^2(3-\alpha)^2}C_1^2C_4^2. \tag{3.33}$$

The result (1.17) now follows using (2.2) and (3.31) in (2.12).

For later reference, it is worth recording the following expressions relevant to the similarity solution in the natural stress basis formulation,

$$\begin{aligned}
\tilde{\lambda}(\xi) &= \frac{t_{11}(\xi)}{f'(\xi)^2}, \\
\tilde{\mu}(\xi) &= t_{12}(\xi) + \frac{t_{11}(\xi)}{f'(\xi)}((3-\alpha)f(\xi) - (2-\alpha)\xi f'(\xi)), \\
\tilde{\nu}(\xi) &= (1+t_{22}(\xi))f'(\xi)^2 + t_{11}(\xi)((3-\alpha)f(\xi) - (2-\alpha)\xi f'(\xi))^2 \\
&\qquad + 2t_{12}(\xi)f'(\xi)((3-\alpha)f(\xi) - (2-\alpha)\xi f'(\xi)).
\end{aligned} \tag{3.34}$$

Using (3.26)–(3.29) gives

$$\tilde{\lambda}(\xi) \sim \frac{C_1}{(3-\alpha)^2 C_0^2}\xi^{-2(2-\alpha)}, \tag{3.35}$$

$$\tilde{\mu}(\xi) \sim \frac{C_1}{2(3-\alpha)C_0}\left(1+\frac{2\alpha(1-\alpha)C_0C_4}{(1+\alpha)}\right)\xi^{-1+\alpha}, \tag{3.36}$$

$$\tilde{\nu}(\xi) \sim \left(\frac{C_1}{4}+\frac{2C_1C_0^2C_5(3-\alpha)(3-2\alpha)}{\alpha}+\frac{(2\alpha^4-5\alpha^3-\alpha^2+9\alpha-9)C_1C_0C_4}{\alpha(1+\alpha)(2-\alpha)}\right.$$
$$\left.+\frac{(\alpha^3-3\alpha^2+4\alpha-3)C_1C_0^2C_4^2}{\alpha}\right)\xi^2 \qquad \text{as } \xi\to\infty. \tag{3.37}$$

It is readily verified that these satisfy

$$\tilde{\lambda}\tilde{\nu}-\tilde{\mu}^2 \sim \Delta_0\xi^{-2+2\alpha} \qquad \text{as } \xi\to\infty \tag{3.38}$$

with Δ_0 as given in (3.33), which is consistent with (3.32).

4. The parametric solution dependence

4.1 The upstream boundary layer

4.1.1 Formulation of the initial value problem

We are interested in solving the fifth order system (3.10)–(3.13) subject to the asymptotic behaviours (3.22) and (3.26)–(3.28). For the upstream boundary layer, we are interested in the case $a<0$, where flow is towards the singularity. Only the third eigenmode in (3.20) is consistent with the asymptotic behaviour (3.22) and corresponds to small changes in the value of a. Imposing the behaviour (3.22) with a specified thus furnishes five boundary conditions for the system (3.10)–(3.13) indicating that it can be solved as an initial value problem (IVP). For a given α, this IVP has only the two freely specifiable parameters (a, p_0) since the parameter b is fixed through the expression (3.18). We thus have a two dimensional parameter space in which to classify solutions that satisfy the far-field behaviour (3.26)–(3.28). This far-field behaviour may be termed generic since it involves the five free constants $(C_0, C_2, C_3, C_4, C_5)$ which have to be determined numerically. It also involves the constant C_1, which is not free but rather fixed since it is related to p_0 directly through (3.23).

For clarity, we now label the constants with an index u in order to distinguish their values from those of the downstream layer. Thus we introduce the identification

$$(a, b, p_0, C_0, C_1, C_2, C_3, C_4, C_5) = (a_u, b_u, p_{0u}, C_{0u}, C_{1u}, C_{2u}, C_{3u}, C_{4u}, C_{5u}). \tag{4.1}$$

In addition we record the explicit expressions for the constants b_u and C_{1u} on a_u and p_{0u}, namely

$$b_u = (1-\alpha)(a_u^2-2p_{0u}), \qquad C_{1u} = 2p_{0u}. \tag{4.2}$$

To facilitate the solution description in terms of the two parameters (a_u, p_{0u}), we note the following scale invariance. The system (3.10)–(3.13) is invariant under the one parameter scaling group

$$\xi = \beta\bar{\xi}, \quad f = \beta\bar{f}, \quad t_{11} = \frac{\bar{t}_{11}}{\beta^2}, \quad t_{12} = \frac{\bar{t}_{12}}{\beta}, \quad t_{22} = \bar{t}_{22}, \tag{4.3}$$

for $\beta \in \mathbb{R}$, whilst for invariance of the wall and far-field asymptotic behaviours (3.22) and (3.26)–(3.28), we require

$$\bar{a}_u = \beta a_u, \qquad \bar{b}_u = \beta^2 b_u, \qquad \bar{p}_{0u} = \beta^2 p_{0u}, \tag{4.4}$$

and

$$\begin{aligned} &\bar{C}_{0u} = \beta^{2-\alpha} C_{0u}, \quad \bar{C}_{1u} = \beta^2 C_{1u}, \quad \bar{C}_{2u} = \beta^{-2+2\alpha} C_{2u}, \\ &\bar{C}_{3u} = \beta^{-1} C_{3u}, \quad \bar{C}_{4u} = \beta^{-2+\alpha} C_{4u}, \quad \bar{C}_{5u} = \beta^{2\alpha-4} C_{5u}. \end{aligned} \tag{4.5}$$

This scaling invariance may be exploited to remove either the parameter a_u or p_{0u} from our system and thus reduce the number of free parameters from two to one. For definiteness, we choose to remove a_u through the choice $\beta = 1/|a_u|$, it now being sufficient to consider the case $a_u = -1$ only.

This scaling invariance may also be used to deduce parameter behaviours as follows. Eliminating β gives

$$\begin{aligned} &\frac{\bar{C}_{0u}}{\bar{p}_{0u}^{1-\frac{\alpha}{2}}} = \frac{C_{0u}}{p_{0u}^{1-\frac{\alpha}{2}}}, \quad \frac{\bar{C}_{1u}}{\bar{p}_{0u}} = \frac{C_{1u}}{p_0}, \quad \frac{\bar{C}_{2u}}{\bar{p}_{0u}^{-1+\alpha}} = \frac{C_{2u}}{p_{0u}^{-1+\alpha}}, \\ &\frac{\bar{C}_{3u}}{\bar{p}_{0u}^{-\frac{1}{2}}} = \frac{C_{3u}}{p_{0u}^{-\frac{1}{2}}}, \quad \frac{\bar{C}_{4u}}{\bar{p}_{0u}^{-1+\frac{\alpha}{2}}} = \frac{C_{4u}}{p_{0u}^{-1+\frac{\alpha}{2}}}, \quad \frac{\bar{C}_{5u}}{\bar{p}_{0u}^{-2+\alpha}} = \frac{C_{5u}}{p_{0u}^{-2+2}}, \end{aligned} \tag{4.6}$$

Now consider solutions in which $a_u = -1$ and $p_{0u} \to +\infty$. Taking $\beta = p_{0u}^{-\frac{1}{2}}$, we can map such solution curves onto the case $\bar{a}_u \to 0^-$ with $\bar{p}_{0u}$ finite. Thus these two limits are equivalent, if they exist and imply that the ratios in (4.6) are finite. We conjecture that such a limit does exist and give numerical evidence to support this later. For the moment then, assuming this conjecture holds we have the following two results:

(a) When $a_u = -1$, as $p_{0u} \to +\infty$ then

$$C_{0u} \sim k_0 p_{0u}^{1-\frac{\alpha}{2}}, \; C_{1u} \sim k_1 p_{0u}, \; C_{2u} \sim \frac{k_2}{p_{0u}^{1-\alpha}}, \; C_{3u} \sim \frac{k_3}{p_{0u}^{\frac{1}{2}}}, \; C_{4u} \sim \frac{k_4}{p_{0u}^{1-\frac{\alpha}{2}}}, \; C_{5u} \sim \frac{k_5}{p_{0u}^{2-\alpha}}. \tag{4.7}$$

(b) For finite p_{0u}, as $a_u \to 0^-$ then

$$C_{0u} \sim k_0 p_{0u}^{1-\frac{\alpha}{2}}, \; C_{1u} \sim k_1 p_{0u}, \; C_{2u} \sim \frac{k_2}{p_{0u}^{1-\alpha}}, \; C_{3u} \sim \frac{k_3}{p_{0u}^{\frac{1}{2}}}, \; C_{4u} \sim \frac{k_4}{p_{0u}^{1-\frac{\alpha}{2}}}, \; C_{5u} \sim \frac{k_5}{p_{0u}^{2-\alpha}}. \tag{4.8}$$

Here, the constants $k_0, k_1, k_2, k_3, k_4, k_5$ have to be found numerically and will depend upon the value of the corner angle parameter α. We in fact already know that $k_1 = 2$ from (4.2) so that that the asymptotic relationship for C_{1u} in (4.7) and (4.8) is exact and holds for all $p_{0u} > 0$ and $a_u < 0$, and not just for p_{0u} large or a_u small.

4.1.2 Numerical scheme for the IVP

Numerical solution of the IVP described in section 4.1.1 is obtained here using MATLAB's stiff solver ode15s. The fifth-order system (3.10)–(3.13) needs to be formulated as a system of first-order equations involving $f, f', t_{11}, t_{12}, t_{22}$. Although implicit systems can be handled by MATLAB's IVP ODE solvers, it is straight forward to form and use an explicit system, which will be of use later when we use the boundary value problem solver bvp4c for the numerical solution of the downstream boundary layer. Using (3.11) and (3.13) in (3.10) gives an equation for $f''(\xi)$, namely

$$f'' = \frac{(1+(\alpha-1)f')(t_{12}-(2-\alpha)\xi t_{11}) + (3-\alpha)\left(\alpha f t_{11} + 2p_0(1-\alpha)f\right)}{((2-\alpha)^2\xi^2 t_{11} - 2(2-\alpha)\xi t_{12} + t_{22} + 1)}, \tag{4.9}$$

which may be used with (3.11)–(3.13) to form our explicit fifth-order system. Since $\xi = 0$ is a singular point for this system we pose the asymptotic behaviour (3.22) at the point $\xi = \xi_0 > 0$ and solve the equations on the finite domain $[\xi_0, \xi_\infty]$ (where, necessarily, ξ_0 needs to be taken small and ξ_∞ suitably large). Specifically, we take one term initial conditions

$$\text{at } \xi = \xi_0 \qquad f = \frac{1}{2}a_u\xi_0^2, \quad f' = a_u\xi_0, \quad t_{11} = 2a_u^2, \quad t_{12} = a_u, \quad t_{22} = 2(1-\alpha)a_u\xi_0, \tag{4.10}$$

where the leading order terms in (3.16) are used. For comparison, two term initial conditions refers to

$$\begin{aligned}\text{at } \xi = \xi_0 \qquad & f = \frac{1}{2}a_u\xi_0^2 + \frac{1}{6}b_u\xi_0^3, \quad f' = a_u\xi_0 + \frac{1}{2}b_u\xi_0^2, \\ & t_{11} = 2a_u^2 + 2a_u(3(1-\alpha)a_u^2 + 2b_u)\xi_0, \quad t_{12} = a_u + 2a_u(3(1-\alpha)a_u^2 + b_u)\xi_0, \\ & t_{22} = 2(1-\alpha)a_u\xi_0 + ((5-4\alpha)(1-\alpha)a_u^2 + (3-2\alpha)b_u)\xi_0^2,\end{aligned} \tag{4.11}$$

where the first two terms in the wall expansion are used. The numerical solution will be sensitive to both the values of ξ_0 and ξ_∞ as well as the number of terms we retain in the expansion (3.16). These effects will be commented upon in the numerical results section below.

4.1.3 Numerical results for the upstream layer

The numerical scheme was implemented in ode15s with the tight error tolerances RelTol= 10^{-13} and AbsTol= 10^{-13}, which are at the limit of sensible values for MATLAB's IVP solvers when working in double precision (see Shampine et al. [13]). To illustrate basic results, we take the benchmark corner angle of 270^o (corresponding to $\alpha = 2/3$) as a representative corner angle.

A) Solution profiles.

For illustration, Figure 2 gives the solution profiles of f and t_{ij} in the parameter case $a_u = -1, p_{0u} = 1, \alpha = 2/3$, where the values $\xi_0 = 10^{-6}$ and $\xi_\infty = 10^6$ were used. Figure 2(A) shows the small ξ behaviour and Figure 2(B) convergence to the leading order far-field asymptotic behaviour (3.15). The legend for Figure 2 gives comparison of the numerical values of the variables at $\xi = \xi_\infty$ and the far-field leading order asymptotic values (which are known since $C_{1u} = 2p_{0u}$ and α are given) and show agreement to four decimal places. Figure 2(C) plots the following rescaled variables

$$\text{Rescaled}\, f = \begin{cases} f, & \xi \leq 1, \\ f\xi^{-(3-\alpha)}, & \xi > 1, \end{cases} \quad \text{Rescaled}\, t_{11} = \begin{cases} t_{11}, & \xi \leq 1, \\ t_{11}, & \xi > 1, \end{cases}$$

$$\text{Rescaled}\, t_{12} = \begin{cases} t_{12}, & \xi \leq 1, \\ t_{12}\xi^{-1}, & \xi > 1, \end{cases} \quad \text{Rescaled}\, t_{22} = \begin{cases} t_{22}, & \xi \leq 1, \\ t_{22}\xi^{-2}, & \xi > 1, \end{cases} \tag{4.12}$$

which remain $O(1)$ and conveniently allow the small and large ξ behaviours to be viewed on the same scale.

B) Estimates of the far-field parameters when $a_u = -1$.

To estimate the far-field constant C_{0u} we use the leading order term for the stream function behaviour in (3.15), namely

$$C^e_{0u} = f(\xi)\xi^{\alpha-3}. \tag{4.13}$$

For the parameter case $a_u = -1, p_{0u} = 1, \alpha = 2/3$, Table 1 in Appendix B records values of this function from the numerical scheme at selected ξ_∞ values. This table also records the sensitivity of the results to both the value of ξ_0 and the number of terms of the expansion (3.22) kept in the initial data. Table 1(A) shows the results when the first terms from (3.22) are kept as stated in (4.10) and Table 1(B) the corresponding results when two terms are used. Convergence is illustrated for fixed ξ_0 with ξ_∞ increasing (i.e. proceeding down the columns) and for fixed ξ_∞ with ξ_0 decreasing (i.e. proceeding across the rows). All values agree to two decimal places. However, for higher accuracy convergence is relatively slow as ξ_∞ increases for fixed ξ_0 (approximately an additional decimal place is gained every two orders of magnitude increase in ξ_∞) and slightly faster as ξ_0 decreases for fixed ξ_∞ (approximately one additional decimal place is gained for each order of magnitude decrease in ξ_0). The effect of including two terms rather than just the first term of the asymptotic expansion (3.22) is more pronounced for the larger ξ_0 values as would be expected e.g. it immediately affects the third decimal place for $\xi_0 = 10^{-2}$, whilst for $\xi_0 = 10^{-6}$ it only affects the seventh. Certainly the adoption of the one term expansion with $\xi_0 = 10^{-6}$ and $\xi_\infty = 10^6$ is sufficient for accuracy to at least four decimal places.

For estimates of the constant C_{2u} we may use each of the stress variables in (3.27)–(3.29) to give three different approximations

$$\begin{aligned} C^{(11)}_{2u} &= \left(\frac{t_{11}(\xi)}{C_{1u}} - 1\right)\frac{(3-\alpha)}{2(2\alpha-1)}\xi^{2-2\alpha}, \\ C^{(12)}_{2u} &= -\left(\frac{t_{12}(\xi)}{C_{1u}(1-\alpha)\xi} - 1\right)\frac{(3-\alpha)}{4(1-\alpha)}\xi^{2-2\alpha}, \\ C^{(22)}_{2u} &= -\left(\frac{t_{22}(\xi)}{C_{1u}(1-\alpha)^2\xi^2} - 1\right)\frac{(3-\alpha)}{2(3-2\alpha)}\xi^{2-2\alpha}. \end{aligned} \tag{4.14}$$

These estimates hold uniformly in α. Estimates of the constant C_{3u} can be obtained from the

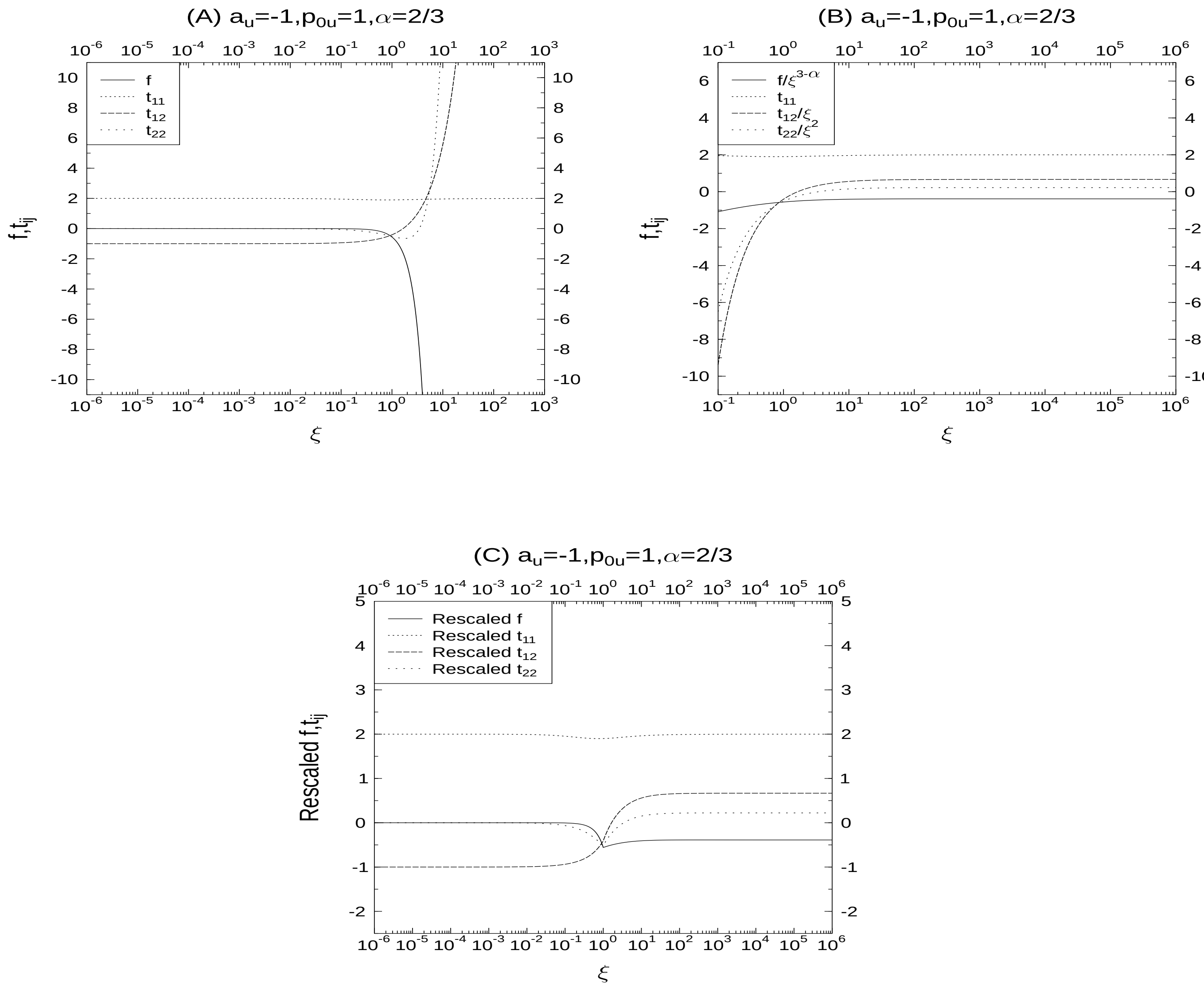

Figure 2: Illustration of the solution to the initial value problem for the case $a_u = -1, p_{0u} = 1, \alpha = 2/3$. Here $\xi_0 = 10^{-6}$ was used. (A) shows the small ξ behaviour and (B) convergence to the leading order far-field asymptotic behaviour (3.15). (C) plots the rescaled variables (4.12), conveniently allowing (A) and (B) to be viewed on the same scale. In (B), the numerical scheme gives the estimates $t_{11}(\xi) = 1.99998228, t_{12}(\xi)/\xi = 0.66667711, t_{22}(\xi)/\xi^2 = 0.22223115$ at $\xi = 10^6$ which compare well with the leading order asymptotic values of these expressions from (3.15) of $C_{1u} = 2p_{0u} = 2, C_{1u}(1-\alpha) = 2/3 = 0.\dot{6}, C_{1u}(1-\alpha)^2 = 2/9 = 0.\dot{2}$ respectively.

stress variables in (3.28) and (3.29) which give the two approximations

$$C_{3u}^{(12)} = -\left(\frac{t_{12}(\xi)}{C_{1u}(1-\alpha)\xi} - 1 + \frac{4(1-\alpha)C_{2u}}{(3-\alpha)}\xi^{-2+2\alpha}\right)(1-\alpha)(3-\alpha)\xi,$$
$$C_{3u}^{(22)} = -\frac{1}{2}\left(\frac{t_{22}(\xi)}{C_{1u}(1-\alpha)^2\xi^2} - 1 + \frac{2(3-2\alpha)C_{2u}}{(3-\alpha)}\xi^{-2+2\alpha}\right)(1-\alpha)(3-\alpha)\xi. \quad (4.15)$$

These expressions provide estimates of C_{3u} as long as $\alpha < 3/4$, otherwise additional terms must included. Also, they require an estimate of C_{2u}, which we obtain from $C_{2u}^{(11)}$. Consistency would indicate that these three estimates of C_{2u} and the two estimates of C_{3u} should be similar. For the parameter case $a_u = -1, p_{0u} = 1, \alpha = 2/3$ and taking one term initial data (4.10) with $\xi_0 = 10^{-6}$, recorded in Table 2 of Appendix B are the values of these five functions at selected ξ_∞. The tabulated values indicate convergence for each of the functions as well consistency between their values. The expressions (4.14) and (4.15) only approximate C_{2u} and C_{3u} respectively at leading order, with different correction terms accounting for differences between the values in the table. The values for C_{3u} are surprisingly consistent given the number of cancelations involved to obtain them.

For estimates of C_{4u} and C_{5u} we use the natural stress variables $\tilde{\lambda}, \tilde{\mu}, \tilde{\nu}$ given by the transformation (3.34), rather than try to extract them from the higher order terms in the Cartesian expansions (3.27)–(3.29). It is straight forward to augment our fifth order system with the three first order ODEs (f being treated as known)

$$(3-\alpha)f\tilde{\lambda}' + (2(2-\alpha)f' - 1)\tilde{\lambda} + 2\frac{f''}{f'^2}\tilde{\mu} = 0, \quad (4.16)$$

$$(3-\alpha)f\tilde{\mu}' + ((1-\alpha)f' - 1)\tilde{\mu} + \frac{f''}{f'^2}\tilde{\nu} = 0, \quad (4.17)$$

$$(3-\alpha)f\tilde{\nu}' - (1+2f')\tilde{\nu} + f'^2 = 0, \quad (4.18)$$

which follow from (3.11)–(3.13) on using (3.34). These are completed with two term initial data

$$\text{at } \xi = \xi_0 \qquad \tilde{\lambda} = 2\xi_0^{-2} + \frac{2}{a_u}(b_u + 3(1-\alpha)a_u^2)\xi_0^{-1},$$
$$\tilde{\mu} = a_u + (b_u + 2(1-\alpha)a_u^2)\xi_0,$$
$$\tilde{\nu} = a_u^2\xi_0^2 + a_u(b_u + (1-\alpha)a_u^2)\xi_0^3, \quad (4.19)$$

which follows from the wall expansion (3.16). Then estimates of $C_{4u}$and C_{5u} can be obtained from (3.36) and (3.37) respectively as

$$C_{4u}^e = \left(\frac{\tilde{\mu}\xi^{1-\alpha}2(3-\alpha)C_{0u}^e}{C_{1u}} - 1\right)\frac{2\alpha(1-\alpha)}{(1+\alpha)C_{0u}^e},$$
$$C_{5u}^e = \left(\tilde{\nu}\xi^{-2} - \frac{C_{1u}}{4} - \frac{(2\alpha^4 - 5\alpha^3 - \alpha^2 + 9\alpha - 9)C_{1u}C_{0u}C_{4u}^e}{\alpha(1+\alpha)(2-\alpha)}\right.$$
$$\left. - \frac{(\alpha^3 - 3\alpha^2 + 4\alpha - 3)C_{1u}(C_{0u}^eC_{4u}^e)^2}{\alpha}\right)\frac{\alpha}{2C_{1u}(C_{0u}^e)^2(3-\alpha)(3-2\alpha)}. \quad (4.20)$$

Table 3 in Appendix B records values of the far-field behaviours of the natural stress variables for this augmented system for the parameter case $a_u = -1, p_{0u} = 1, \alpha = 2/3$ with $\xi_0 = 10^{-6}$

and selected ξ_∞ values. The first two columns illustrate convergence to the far-field behaviour (3.35), whilst columns three and four show convergence to the behaviours (3.36) and (3.37). The last two columns give the estimates of C_{4u} and C_{5u} using (4.20), the estimate of C_{4u} appearing to converge to zero.

Figure 3(A) and (B) illustrate the behaviour of the estimates of the far-field parameters $C_{0u}, C_{2u}, C_{3u}, C_{4u}, C_{5u}$ in the case $a_u = -1, \alpha = 2/3$ for $p_{0u} > 0$. The numerical scheme used $\xi_0 = 10^{-6}$ with estimates $C^e_{0u}, C^{11}_{2u}, C^{12}_{3u}, C^e_{4u}, C^e_{5u}$ evaluated at $\xi_\infty = 10^6$. It is noteworthy that the values of C^e_{4u} seem to imply that $C_{4u} = 0$ for $p_{0u} > 0$. This considerably simplifies the expressions in (3.26)–(3.29), (3.33) as well as (3.36) and (3.37). Shown in Figure 3(C) are estimates of C_{0u} over a range of p_{0u} for selected values of the re-entrant corner angle parameter α. It is clear that the curves in Figure 3(C) do not appear to behave in a monotonic manner with respect to α over the whole of the range of p_{0u}.

C) Estimates of constants k_i in (4.7) and (4.8).

Numerical evidence of the behaviours (4.7) is recorded in Table 4 in Appendix B in the parameter case $a_u = -1, \alpha = 2/3$. There the values of $C^e_{0u}, C^{11}_{2u}, C^{12}_{3u}, C^e_{4u}, C^e_{5u}$ are used as estimates for their corresponding far-field parameters each multiplied by the appropriate power of p_{0u} and evaluated at selected large p_{0u} values. The scheme parameters were one term initial data with $\xi_0 = 10^{-6}$ and $\xi_\infty = 10^6$. Convergence with increasing p_{0u} is indicated supporting the conjecture that the limits (4.7) and (4.8) exist. In keeping with the numerical evidence that $C_{4u} = 0$ we have also that $k_4 = 0$. No satisfactorily stable estimates of k_3 were obtained.

It is natural to ask how fast do the coefficients approach the large p_{0u} asymptotic behaviour. As an indication, for fixed parameters $a_u = -1, \alpha = 2/3$, the relative percentage error between the numerical estimate C^{num}_{0u} of C_{0u} and the asymptotic approximation $C^{asy}_{0u} = k_0 p_0^{2-\alpha}$, defined as

$$\frac{C^{asy}_{0u} - C^{num}_{0u}}{C^{num}_{0u}} \times 100\%$$

is monotonic decreasing with p_{0u}. It is 50% when $p_{0u} \approx 1.1$, 10% for $p_{0u} \approx 10$, 5% when $p_{0u} \approx 21$, 1% when $p_{0u} \approx 130$ indicating a relatively fast convergence.

Figure 4 gives the behaviour of the constants k_0, k_2, k_4 and k_5 with the corner angle α for the parameter case $a_u = -1$ where the numerical scheme used $\xi_0 = 10^{-6}, \xi_\infty = 10^6$ and $p_{0u} = 10^6$. The constants k_0, k_4, k_5 do not change appreciably over most of the range of α in contrast to k_2. The estimates for α close to 1 (e.g. for $\alpha > 0.9$) should be viewed cautiously, where loss of accuracy starts to take place.

D) Estimates of the far-field parameters when $a_u \neq -1$.

For a given re-entrant corner angle α, the parameter behaviours of the far-field constants in the case of other a_u values can be obtained from the $a_u = -1$ case through use of the scaling invariance given by (4.4) and (4.5). Specifically, if we have the values

$$p_{0u} = \hat{p}_{0u}, \quad C_{0u} = \hat{C}_{0u}, \quad C_{1u} = \hat{C}_{1u} \quad C_{2u} = \hat{C}_{2u}, \quad C_{3u} = \hat{C}_{3u}, \quad C_{4u} = \hat{C}_{4u}, \quad C_{5u} = \hat{C}_{5u}, \tag{4.21}$$

when $a_u = -1$, then we obtain

$$p_{0u} = (-a_u)^2 \hat{p}_{0u} \quad C_{0u} = (-a_u)^{2-\alpha} \hat{C}_{0u}, \quad C_{1u} = (-a_u)^2 \hat{C}_{1u} \quad C_{2u} = (-a_u)^{-2+2\alpha} \hat{C}_{2u},$$

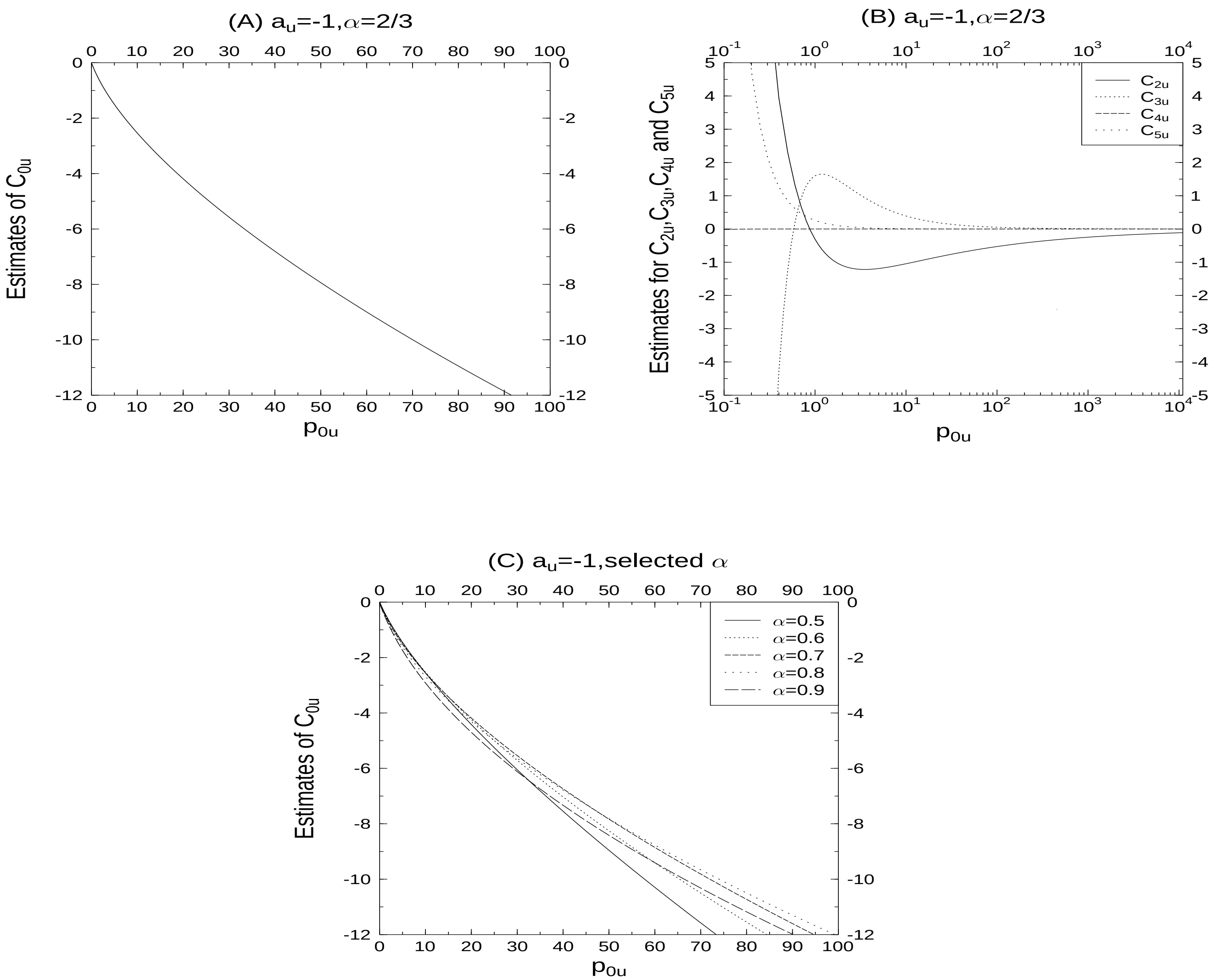

Figure 3: (A) and (B) illustrate estimates of the far-field parameters $C_{0u}, C_{2u}, C_{3u}, C_{4u}, C_{5u}$ in the case $a_u = -1, \alpha = 2/3$ for $p_{0u} > 0$. The numerical scheme used $\xi_0 = 10^{-6}$ with estimates $C^e_{0u}, C^{11}_{2u}, C^{12}_{3u}, C^e_{4u}, C^e_{5u}$ evaluated at $\xi_\infty = 10^6$. It is noteworthy that numerically we obtain $C^e_{4u} \approx 0$. Shown in (C) are estimates of C_{0u} over a range of p_{0u} for selected values of the re-entrant corner angle parameter α.

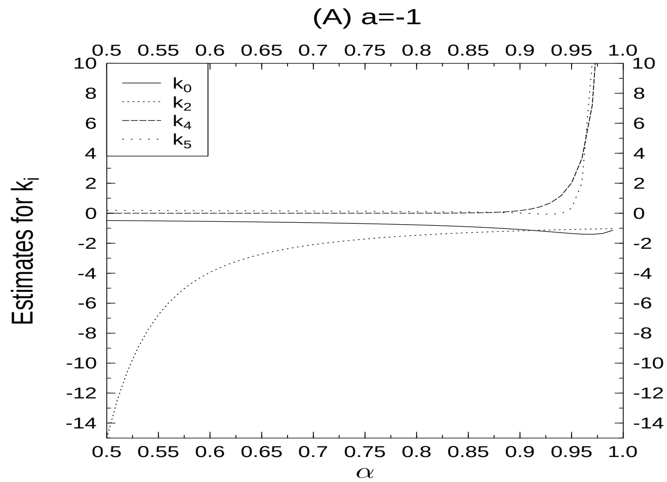

Figure 4: Illustration of the estimates of k_0, k_2, k_4, k_5 with re-entrant corner angle α. The initial value problem was solved using the parameters $a_u = -1, p_{0u} = 10^6, \xi_0 = 10^{-6}, \xi_\infty = 10^6$.

$$C_{3u} = (-a_u)^{-1}\hat{C}_{3u}, \quad C_{4u} = (-a_u)^{-2+\alpha}\hat{C}_{4u}, \quad C_{5u} = (-a_u)^{-4+2\alpha}\hat{C}_{5u}, \tag{4.22}$$

for other $a_u < 0$ values.

However, it is still beneficial to plot the parameter curves over a range of a_u values to observe their sensitivity to a_u and the existence of the limit curves as $a_u \to 0^-$. Figure 5 shows the variation of the estimates of the parameters $C_{0u}, C_{2u}, C_{3u}, C_{5u}$ with p_{0u} for selected a_u values when $\alpha = 2/3$. The scheme parameters were one term initial data with $\xi_0 = 10^{-6}, \xi_\infty = 10^6$. Figure 5(A) shows C_{0u} estimates, where the $a_u = -0.01$ and $a_u = -0.1$ curves are visibly indistinguishable. For a given pressure gradient, this corresponds to there being a minimum value for the coefficient of the stream function which has already been remarked upon by [7]. However, here we taken the analysis one step further, where (4.8) gives an analytic expression for such a curve. The estimate $k_0 = -0.5989$ from Table 4 in Appendix A when used in the expression for C_{0u} in (4.8) provides an extremely good fit to the $a_u = -0.01$ numerical curve given in Figure 5(A). The other limit of note is $a_u \to -\infty$ in which we obtain $C_{0u} \to 0^-$ uniformly in p_{0u}, which seems to be supported by the numerical evidence. In Figure 5(B)–(D), the $a_u = -0.01$ curve provides a very good approximation to the limit curves of (4.8) at least for $p_{0u} > 10^{-3}$ (it does in fact start deviating for smaller p_{0u} values).

E) The case $a_u = 0$.

In this case we have explicit expressions for all of the parameters in terms of p_{0u}. Using (4.2)

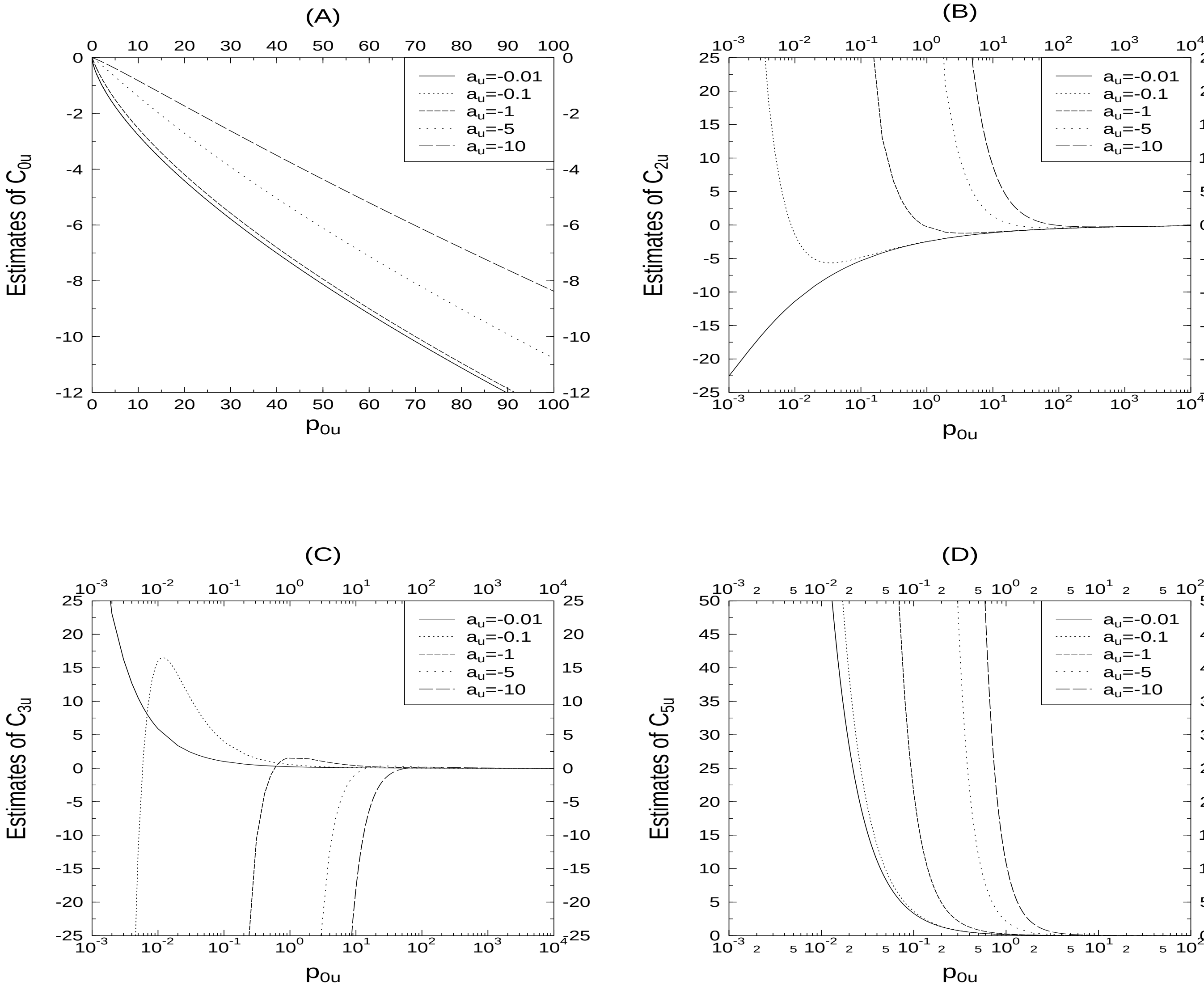

Figure 5: Estimates of $C_{0u}, C_{2u}, C_{3u}, C_{4u}$ against p_{0u} in the case $\alpha = 2/3$ for selected a_u. The IVP used the parameters $\xi_0 = 10^{-6}, \xi_\infty = 10^6$. The $a_u \neq -1$ curves are related to the $a_u = -1$ curves through the scalings (4.22).

and (4.8), these are

$$b_u = -2(1-\alpha)p_{0u}, \quad C_{0u} = k_0 p_{0u}^{1-\frac{\alpha}{2}}, \quad C_{1u} = 2p_{0u},$$
$$C_{2u} = \frac{k_2}{p_{0u}^{1-\alpha}}, \quad C_{3u} = \frac{k_3}{p_{0u}^{\frac{1}{2}}}, \quad C_{4u} = \frac{k_4}{p_{0u}^{1-\frac{\alpha}{2}}}, \quad C_{5u} = \frac{k_5}{p_{0u}^{2-\alpha}}. \tag{4.23}$$

Numerically, we have seen that $k_4 = 0$ and relevant to the natural stress basis are the behaviours of C_{0u} and C_{5u}. In both cases, these curves provide extreme bounds on the values of these constants. Specifically, for a given value of p_{0u} we obtain the minimum values of both C_{0u} and C_{5u} in the case $a_u = 0$ when compared to $a_u < 0$. Interestingly, [7] conjecture that these extreme values of C_{0u} are those that occur in the presence of the separating streamline at the upstream wall when a lip vortex is present.

4.2 The downstream boundary layer

4.2.1 Formulation of the boundary value problem

The downstream boundary layer can be considered in direct analogous fashion to that of the upstream case. Remark 3 in the introduction indicates that the majority of the set up and analysis of section 3 carries over. Consequently equations (3.3)–(3.6) hold, the essential difference being in the sign of the stream function which must be positive for the downstream stream case i.e. we are now considering flow away from the singularity. The boundary layer equations in similarity variables (3.10)–(3.13) hold, as do the far-field behaviours (3.26)–(3.28) and the local wall expansion (3.16) to the order recorded. However, the cases $C_0 > 0$ and $a > 0$ are now of relevance, and thus it should be noted that stream function and extra-stress variables are no longer analytic at the downstream wall, the full wall behaviour actually containing exponentially small terms as given in (3.22). The wall behavior thus contains three free parameters a, K_1, K_2 although it will not be possible to impose or determine numerically the parameters K_1, K_2. The constant b is fixed, being related to a and p_0 through (3.18). The far-field behaviour again involves the six parameters $(C_0, C_1, C_2, C_3, C_4, C_5)$, where C_1 is related to p_0 through (3.23).

Following the upstream case, for clarity we label these parameters with an index d in order to distinguish them from those of the upstream layer. Thus we introduce the identification

$$(a, b, p_0, C_0, C_1, C_2, C_3, C_4, C_5) = (a_d, b_d, p_{0d}, C_{0d}, C_{1d}, C_{2d}, C_{3d}, C_{4d}, C_{5d}).$$

Numerical solution of (3.10)–(3.13) subject to (3.26)–(3.28) and (3.22) needs to be considered as a two-point boundary value problem (BVP). The main reason for this is the presence of the essential singularity of the governing equations at the downstream wall containing two degrees of freedom (through K_1 and K_2). Thus at most three conditions can be imposed through the specification of the local asymptotic behaviour (3.16) (to be precise, two boundary conditions if $a = a_d$ is left unspecified or three if it is specified). This could also be argued physically where due to the hyperbolic nature of the governing equations, the downstream boundary layer is expected to receive information from the outer core solution as the fluid sweeps in to the downstream wall, as well as having to satisfy the conditions of no slip on the downstream wall. There are in fact several ways to formulate the downstream BVP, which we now discuss.

1. Formulation BVP1: specify $(p_{0d}, a_d, C_{0d}, C_{2d})$. Here the necessary five boundary conditions are imposed as three at the wall and two in the far-field. This may be explained as follows. The specification of a_d in the wall behaviour (3.16) or (3.22) imposes three boundary conditions, as verified by the inconsistency of the first three modes in (3.20) (i.e. it removes these three modes). The specification of C_{0d} and C_{2d} in (3.26)–(3.28) removes the first and second modes in (3.25) and thus together impose two conditions. The parameter p_{0d} needs to be specified as a parameter of the equations (3.10)–(3.13) and thus C_{1d} is then determined (and which doesn't impose any further conditions in the far-field due to the lack of an eigenmode associated with small changes in the value of C_{1d}).

2. Formulation BVP2: specify $(p_{0d}, C_{0d}, C_{4d}, C_{5d})$. Now we have two conditions being imposed at the wall and three in the far-field. Here a_d is left unspecified (in (3.16) or (3.22)) and thus only the first two modes in (3.20) are now removed. The specification of C_{0d}, C_{4d}, C_{5d} removes the first, fourth and fifth modes in (3.25) and thus imposes three conditions. Again p_{0d} is assumed specified which is equivalent to specifying C_{1d} (which does not impose an additional condition).

In both these formulations, the parameters left unspecified are determined as part of the solution and can in principle be obtained numerically (apart from K_1, K_2). BVP2 is one of several formulations in which three conditions are imposed in the far-field and the downstream wall shear rate a_d is to be determined. Another obvious one being to specify $(p_{0d}, C_{0d}, C_{2d}, C_{3d})$. To discuss the merits of the above two formulations it is first worth recording the relationships between the upstream and downstream far-field parameters

$$p_{0u} = p_{0d}, \quad C_{0u} = -C_{0d}, \quad C_{1u} = C_{1d}, \quad C_{4u} = -C_{4d}, \quad C_{5u} = C_{5d}. \tag{4.24}$$

These relationships follow from the core outer solution (2.7)–(2.8) with (2.10), together with the necessary sign transformation relating the upstream and downstream layers as described in Remark 3 of the introduction. The transmission of the values of C_{1u}, C_{4u}, C_{5u} to the downstream layer follows from the natural stress variables being constant at leading order along streamlines (see [7] and [5]). Consequently BVP2 is the formulation in which information from the upstream layer can be related and used in the downstream layer. However, this formulation is better posed using the natural stress variables rather than the Cartesian stresses due to the high term cancelations needed in the far-field of the latter. We thus leave further parameter description of downstream layer solution until [5].

It is worth remarking that formulation BVP1 is not without merit, particularly in the more general setting when fluid entering the downstream layer no longer originates from the upstream near wall region. The advantages are that it is well suited to the Cartesian formulation and can be used to demonstrate numerical solutions of the boundary layer equations. Its disadvantage in the current setting is that it is no longer clear how the downstream parameters (specifically a_d, C_{2d}) are related to the upstream parameters. For completeness, we discuss a numerical scheme for the BVP1 below.

As for the upstream layer, the downstream layer problem has a scale invariance described through the one parameter scaling group (4.3) with invariance of the wall and far-field asymptotic behaviours (3.22) and (3.26)–(3.28) requiring

$$\bar{a}_d = \beta a_d, \quad \bar{b}_d = \beta^2 b_d, \quad \bar{p}_{0d} = \beta^2 p_{0d}, \quad \bar{K}_1 = \beta^{q_1+4} K_1, \quad \bar{K}_2 = \beta^{q_2+2} K_2, \tag{4.25}$$

and

$$\bar{C}_{0d} = \beta^{2-\alpha}C_{0d}, \quad \bar{C}_{1d} = \beta^2 C_{1d}, \quad \bar{C}_{2d} = \beta^{-2+2\alpha}C_{2d}, \quad \bar{C}_{3d} = \beta^{-1}C_{3d},$$
$$\bar{C}_{4d} = \beta^{-2+\alpha}C_{4d}, \quad \bar{C}_{5d} = \beta^{2\alpha-4}C_{5d}. \tag{4.26}$$

This scaling invariance may be exploited in the following ways:

1. The choice $\beta = (\bar{p}_{0d})^{1/2}$ means that the normalized case $p_{0d} = 1$ can always be considered for the downstream layer (or alternatively $a_d = 1$ if $\beta = \bar{a}_d$).

2. Suppose that we have the values

$$p_{0d} = \hat{p}_{0d}, \quad a_d = \hat{a}_d, \quad b_d = \hat{b}_d, \quad , \quad K_{1d} = \hat{K}_{1d}, \quad K_{2d} = \hat{K}_{2d},$$
$$C_{0d} = \hat{C}_{0d}, \quad C_{1d} = \hat{C}_{1d}, \quad C_{2d} = \hat{C}_{2d}, \quad C_{3d} = \hat{C}_{3d}, \quad C_{4d} = \hat{C}_{4d}, \quad C_{5d} = \hat{C}_{5d}, \tag{4.27}$$

for example from solution of BVP2 (admittedly, only theoretically in the case of K_1, K_2), where in fact

$$\hat{p}_{0d} = \hat{p}_{0u}, \quad \hat{C}_{0d} = -\hat{C}_{0u}, \quad \hat{C}_{1d} = \hat{C}_{1u}, \quad \hat{C}_{4d} = -\hat{C}_{4u}, \quad \hat{C}_{5d} = \hat{C}_{5u},$$

with the upstream values corresponding to the solution of the upstream case $a_u = -1$ with fixed re-entrant corner angle α as in (4.21). Complementing (4.22), the downstream parameter values for the case of other $a_u < 0$ values can be deduced as

$$p_{0d} = (-a_u)^2\hat{p}_{0d}, \ a_d = (-a_u)\hat{a}_d, \ b_d = (-a_u)^2\hat{b}_d, \ K_{1d} = (-a_u)^{q_1+4}\hat{K}_{1d}, \ K_{2d} = (-a_u)^{q_2+2}\hat{K}_{2d},$$
$$C_{0d} = (-a_u)^{2-\alpha}\hat{C}_{0d}, \quad C_{1d} = (-a_u)^2\hat{C}_{1d}, \quad C_{2d} = (-a_u)^{-2+2\alpha}\hat{C}_{2d},$$
$$C_{3d} = (-a_u)^{-1}\hat{C}_{3d}, \quad C_{4d} = (-a_u)^{-2+\alpha}\hat{C}_{4d}, \quad C_{5d} = (-a_u)^{-4+2\alpha}\hat{C}_{5d}. \tag{4.28}$$

3. Relevant to BVP2, complementing (4.7) and (4.8), we have

(A) When $a_u = -1$, as $p_{0u} = p_{0d} \to +\infty$ then (4.7) and (4.24) give

$$C_{0d} \sim -k_0 p_{0d}^{1-\frac{\alpha}{2}}, \ C_{1d} = \frac{1}{2}p_{0d}, \ C_{4d} \sim -\frac{k_4}{p_{0d}^{1-\frac{\alpha}{2}}}, \ C_{5u} \sim \frac{k_5}{p_{0d}^{2-\alpha}}, \ a_d \sim k_d p_{0d}^{1/2}. \tag{4.29}$$

(b) For finite $p_{0u} = p_{0d}$, as $a_u \to 0^-$ then (4.8) and (4.24) give

$$C_{0d} \sim -k_0 p_{0d}^{1-\frac{\alpha}{2}}, \ C_{1d} = \frac{1}{2}p_{0d}, \ C_{4d} \sim -\frac{k_4}{p_{0d}^{1-\frac{\alpha}{2}}}, \ C_{5u} \sim \frac{k_5}{p_{0d}^{2-\alpha}}, \ a_d \sim k_d p_{0d}^{1/2}. \tag{4.30}$$

The behaviour for a_d can be deduced from (4.26), where k_d is an additional constant and numerical values of which are given when we consider the natural stress basis formulation in [5].

4.2.2 Numerical scheme for BVP1

Numerical solution of BVP1 (which was described in section 4.2.1) may be obtained using MATLAB's boundary value solver bvp4c. The fifth-order system (3.10)–(3.13) is formulated as an explicit system of first-order equations involving as described in section 4.1.2 and considered on the finite interval $[\xi_0, \xi_\infty]$. For boundary conditions we impose

$$\text{at } \xi = \xi_0 \qquad f = \frac{1}{2}a_d\xi_0^2, \quad t_{12} = a_d, \tag{4.31}$$

$$\begin{aligned}\text{at } \xi = \xi_\infty \qquad & f = C_{0d}\xi_\infty^{3-\alpha}\left(1 + C_{2d}\xi_\infty^{-2+2\alpha}\right), \quad f' = (3-\alpha)C_{0d}\xi_\infty^{2-\alpha} + (1+\alpha)C_{0d}C_{2d}\xi_\infty^{\alpha},\\ & t_{11} = C_{1d}\left(1 + \frac{2(2\alpha-1)C_{2d}}{(3-\alpha)}\xi_\infty^{-2+2\alpha}\right).\end{aligned} \tag{4.32}$$

The solver bvp4c is implemented with error tolerances RelTol$= 10^{-6}$,AbsTol$= 10^{-6}$, vectorization and an initial solution guess

$$f = \begin{cases} \frac{1}{2}a_d\xi^2 + (C_{0d} - \frac{1}{2}a_d)\xi^3, & \xi \le 1,\\ C_{0d}\xi^{(3-\alpha)}, & \xi > 1,\end{cases} \qquad f' = \begin{cases} a_d\xi + (C_{0d}(3-\alpha) - a_d)\xi^2, & \xi \le 1,\\ C_{0d}(3-\alpha)\xi^{(2-\alpha)}, & \xi > 1,\end{cases}$$

$$t_{11} = \begin{cases} 2a_d^2 + (C_{1d} - 2a_d^2)\xi, & \xi \le 1,\\ C_{1d}, & \xi > 1,\end{cases} \qquad t_{12} = \begin{cases} a_d + (C_{1d}(1-\alpha) - a_d)\xi, & \xi \le 1,\\ C_{1d}(1-\alpha)\xi, & \xi > 1,\end{cases}$$

$$t_{22} = \begin{cases} 2(1-\alpha)a_d\xi + (C_{1d}(1-\alpha)^2 - 2(1-\alpha)a_d)\xi^2, & \xi \le 1,\\ C_{1d}(1-\alpha)^2\xi^2, & \xi > 1.\end{cases}$$

The initial guess solution is posed on a reduced interval with $\xi_0 = 10^{-1}, \xi_\infty = 10$ using 200 equally spaced mesh points. Continuation with MATLAB's bvpinit is used to extend the solution to an interval with $\xi_0 = 10^{-4}, \xi_\infty = 10^4$. Purely as an illustration, Figure 6 shows the solution profile in the parameter case $(a_d, C_{0d}, C_{1d}, C_{2d}) = (1, 0.3435, 2 \times 0.8738, 0)$ with $\alpha = 2/3$.

5. Discussion

This paper is the first of a pair describing the local asymptotic solution for the flow of UCM fluids around a re-entrant corner as a two parameter family for each fixed re-entrant corner angle. The two parameters used are a_u and p_{0u} these being the upstream coefficients of the wall shear rate and near wall pressure gradient respectively. The local stream function and pressure behaviour at the upstream wall is

$$\psi \sim \frac{1}{2}a_u x^{\alpha-1}y^2, \qquad p \sim p_{0u}x^{2(\alpha-1)} \qquad \text{as } y \to 0, x \to 0,$$

so that the wall shear rate is $a_u x^{\alpha-1}$ and pressure gradient is $2(\alpha-1)p_{0u}x^{2\alpha-3}$. The choice of these two parameters is not unique and any pair from the triple (a_u, b_u, p_{0u}) could be used. There is no unique relationship relating the leading order stream function and stress behaviours i.e. the coefficients C_{0u} and C_{1u} are independent. A full investigation of the parameter dependence of the upstream boundary layer has been given, with that for the downstream layer being completed in the companion paper [5]. It is worth noting that the analysis presented here breaks down

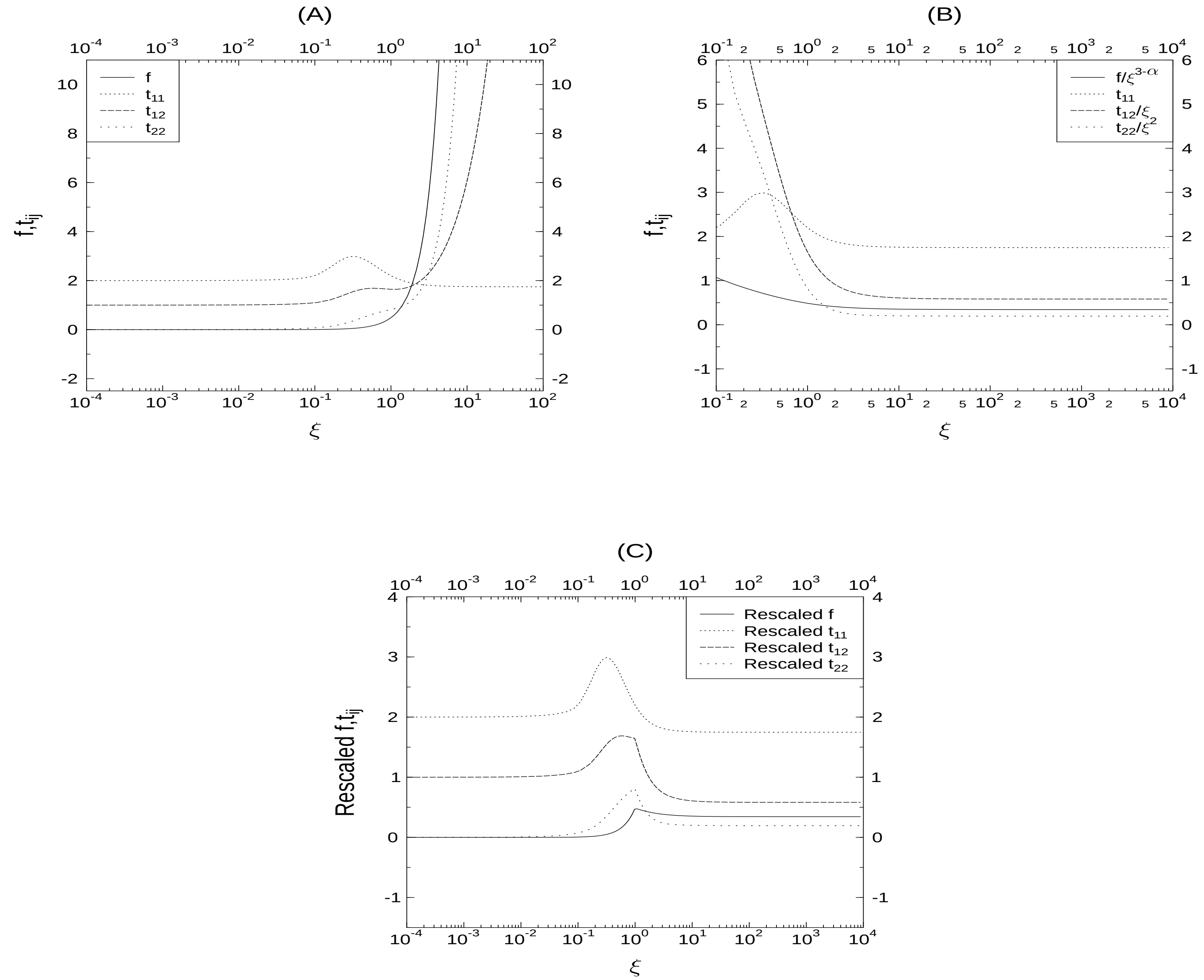

Figure 6: Illustration of the solution to the boundary value problem BVP1 for the case $(C_0, C_1, C_2, C_4) = (0.3435, 2 \times 0.8738, 0, 0.323)$. Parameter values chosen were $\alpha = 2/3, \xi_0 = 10^{-4}, \xi_\infty = 10^4$. (A) shows convergence to the small ξ behaviour and (B) the large ξ behaviour suitably scaled with the leading order far-field asymptotic behaviour. (C) plots the rescaled variables (4.12), conveniently allowing (A) and (B) to be viewed on the same scale.

when $\alpha = 1$, where the stress singularity is no longer present and that the limit $\alpha \to 1^-$ appears non-uniform.

Importantly, the analysis has showed the interplay between the Cartesian and natural stress bases, and in particular the remarkable way in which the natural stress basis un picks the Cartesian solution behaviour extracting information from high order terms. The benefit of using the natural stress basis is now apparent and in particular allows the upstream and downstream boundary layers to be linked directly.

Finally it is worth remarking upon the case when a lip vortex is present at the upstream wall. If the separating streamline makes an angle π/α' with the upstream wall then we again have an effective re-entrant corner if $\pi/\alpha - \pi/\alpha' > \pi$. In this case the leading order outer solution and the downstream boundary layer would still be expected to be the same. Now, however, the fluid entering the outer region comes from a mainstream flow for which a greater variety of conditions would be anticipated to exist than when it originates at the upstream wall. In this case, either of the formulations BVP1 or BVP2 would be suitable to demonstrate solutions at the downstream wall, where we would need to cover greater parameter ranges. For example, in BVP2, the case $C_4 = C_{4d} \neq 0$ would now be expected to arise. Alternatively, if $\pi/\alpha - \pi/\alpha' = \pi$, then the analysis presented here will not by relevant.

References

[1] J.D. Evans, Re-entrant corner flows of the Upper Convected Maxwell fluid. *Proc. Roy. Soc. A*, **461** (2005), 117–142.

[2] J.D. Evans, Re-entrant corner flows of UCM fluids: The small and high Weissenberg number limits. *Submitted to Proc. Roy. Soc. A*, (2005).

[3] J.D. Evans, Re-entrant corner flows of Oldroyd-B fluids. *Proc. Roy. Soc. A*. **461** (2005), 2573-2603.

[4] J.D. Evans, Re-entrant corner flows of UCM fluids: The initial formation of lip vortices. *Proc. Roy. Soc. A*. **461** (2005), 3169-3181.

[5] J.D. Evans, Re-entrant corner flows of UCM fluids: The natural stress basis. *Submitted to J. Non-Newtonian Fluid Mech.* (2006).

[6] E.J. Hinch, The flow of an Oldroyd fluid around a sharp corner. *J. Non-Newtonian Fluid Mech.* **50** (1993), 161–171.

[7] J.M. Rallison and E.J. Hinch, The flow of an Oldroyd fluid past a reentrant corner: the downstream boundary layer. *J. Non-Newtonian Fluid Mech.* **116** (2004), 141–162.

[8] M. Renardy, How to integrate the upper convected Maxwell (UCM) stresses near a singularity (and maybe elsewhere,too). *J.Non-Newtonian Fluid Mech.* **52** (1994), 91–95.

[9] M. Renardy, A matched solution for corner flow of the upper convected Maxwell fluid. *J.Non-Newtonian Fluid Mech.* **58** (1995), 83–39.

[10] M. Renardy, High Weissenberg number boundary layers for the upper convected Maxwell fluid. *J. Non-Newtonian Fluid Mech.* **68** (1997), 125–132.

[11] M. Renardy, The high Weissenberg number limit of the UCM model and the Euler equations. *J. Non-Newtonian Fluid Mech.* **69** (1997), 293–301.

[12] M. Renardy, *Mathematical Analysis of Viscoelastic Flows.* SIAM, 2000.

[13] L.E. Shampine, I. Gladwell and S. Thompson, *Solving ODEs with MATLAB.* CUP, 2003.

Appendix A. The case $a = 0$

A local analysis at $\xi = 0$, for viscometric behaviour in this case, shows that

$$
\begin{aligned}
f(\xi) &= \frac{1}{3!}b\xi^3 - \frac{1}{7!}8\alpha(3-2\alpha)b^3\xi^7 + O(\xi^8),\\
t_{11}(\xi) &= 2b^2\xi^2 + 2(3-2\alpha)b^3\xi^4 + O(\xi^6),\\
t_{12}(\xi) &= b\xi - \frac{4}{3}(3-2\alpha)b^2\xi^3 + \frac{4}{5}(3-2\alpha)(5-3\alpha)b^3\xi^5 + O(\xi^6),\\
t_{22}(\xi) &= (3-2\alpha)b\xi^2 + \frac{1}{3}(3-2\alpha)(8-5\alpha)b^2\xi^4 + O(\xi^6),
\end{aligned}
\tag{A.1}
$$

where $b = f'''(0)$, and

$$
p_0 = \frac{1}{2(\alpha-1)}b. \tag{A.2}
$$

In this case, following (3.19) with (A.1) being used for $f^{(0)}, t_{ij}^{(0)}$, the eigenmodes in place of (3.20) are now

$$
\left.\begin{aligned}
\hat f &\sim 1\\
\hat t_{11} &\sim 6(3-\alpha)b^2\xi\\
\hat t_{12} &\sim (3-\alpha)b\\
\hat t_{22} &\sim 2(3-\alpha)(1-\alpha)b
\end{aligned}\right\};\quad
\left.\begin{aligned}
\hat f &\sim \xi\\
\hat t_{11} &\sim 4(4-\alpha)b^2\xi^2\\
\hat t_{12} &\sim -\tfrac{8}{3}(3-2\alpha)(4-\alpha)b^2\xi^3\\
\hat t_{22} &\sim -2
\end{aligned}\right\};\quad
\left.\begin{aligned}
\hat f &\sim \xi^2\\
\hat t_{11} &\sim 8b\xi\\
\hat t_{12} &\sim 2\\
\hat t_{22} &\sim 4(1-\alpha)\xi
\end{aligned}\right\};
$$

$$
\left.\begin{aligned}
\hat f &\sim \xi^{q_1+7}\exp\left(-\tfrac{3}{b(3-\alpha)\xi^2}\right)\\
\hat t_{11} &\sim \tfrac{72}{(3-\alpha)^3b^2}\xi^{q_1}\exp\left(-\tfrac{3}{b(3-\alpha)\xi^2}\right)\\
\hat t_{12} &\sim \tfrac{72(2-\alpha)}{(3-\alpha)^3b^2}\xi^{q_1+1}\exp\left(-\tfrac{3}{b(3-\alpha)\xi^2}\right)\\
\hat t_{22} &\sim -\tfrac{36}{(3-\alpha)^2b^3}\xi^{q_1}\exp\left(-\tfrac{3}{b(3-\alpha)\xi^2}\right)
\end{aligned}\right\};\quad
\left.\begin{aligned}
\hat f &= o\left(\xi^{q_2+8}\exp\left(-\tfrac{3}{b(3-\alpha)\xi^2}\right)\right)\\
\hat t_{11} &\sim \xi^{q_2}\exp\left(-\tfrac{3}{b(3-\alpha)\xi^2}\right)\\
\hat t_{12} &\sim (2-\alpha)\xi^{q_2+1}\exp\left(-\tfrac{3}{b(3-\alpha)\xi^2}\right)\\
\hat t_{22} &= (2-\alpha)^2\xi^{q_2+2}\exp\left(-\tfrac{3}{b(3-\alpha)\xi^2}\right)
\end{aligned}\right\}; \tag{A.3}
$$

where

$$
q_1 = \frac{6}{(3-\alpha)}, \qquad q_2 = -6\frac{(2-\alpha)}{(3-\alpha)}. \tag{A.4}
$$

The first three modes are always inconsistent with the asymptotic behaviour (A.1), whereas the behaviour of the fourth and fifth modes depend crucially on the sign of b. They are exponentially large and inconsistent with the expansion (3.16) if $b < 0$ whereas they are both exponentially small and consistent if $b > 0$.

Appendix B. Tables of numerical results for the upstream layer

(A) 1 term initial data

	$\xi_0 = 10^{-2}$	$\xi_0 = 10^{-3}$	$\xi_0 = 10^{-4}$	$\xi_0 = 10^{-5}$	$\xi_0 = 10^{-6}$
ξ_∞	C^e_{0u}	C^e_{0u}	C^e_{0u}	C^e_{0u}	C^e_{0u}
10^2	-0.38768655	-0.38842671	-0.38850087	-0.38850828	-0.38850902
10^3	-0.38691663	-0.38795288	-0.38805670	-0.38806708	-0.38806812
10^4	-0.38725666	-0.38836623	-0.38847738	-0.38848850	-0.38848961
10^5	-0.38738750	-0.38851382	-0.38862664	-0.38863793	-0.38863905
10^6	-0.38742177	-0.38855179	-0.38866498	-0.38867630	-0.38867743
10^7	-0.38742977	-0.38856061	-0.38867387	-0.38868520	-0.38868633
10^8	-0.38743156	-0.38856257	-0.38867585	-0.38868718	-0.38868832
10^9	-0.38743195	-0.38856300	-0.38867629	-0.38868762	-0.38868875
10^{10}	-0.38743204	-0.38856309	-0.38867638	-0.38868771	-0.38868884

(B) 2 term initial data

	$\xi_0 = 10^{-2}$	$\xi_0 = 10^{-3}$	$\xi_0 = 10^{-4}$	$\xi_0 = 10^{-5}$	$\xi_0 = 10^{-6}$
ξ_∞	C^e_{0u}	C^e_{0u}	C^e_{0u}	C^e_{0u}	C^e_{0u}
10^2	-0.38851736	-0.38850919	-0.38850911	-0.38850911	-0.38850911
10^3	-0.38807978	-0.38806835	-0.38806824	-0.38806823	-0.38806823
10^4	-0.38850209	-0.38848985	-0.38848973	-0.38848973	-0.38848973
10^5	-0.38865173	-0.38863930	-0.38863918	-0.38863918	-0.38863918
10^6	-0.38869015	-0.38867769	-0.38867756	-0.38867756	-0.38867756
10^7	-0.38869906	-0.38868659	-0.38868646	-0.38868646	-0.38868646
10^8	-0.38870104	-0.38868857	-0.38868844	-0.38868844	-0.38868844
10^9	-0.38870147	-0.38868900	-0.38868888	-0.38868888	-0.38868888
10^{10}	-0.38870157	-0.38868910	-0.38868897	-0.38868897	-0.38868897

Table 1: Estimates of the upstream boundary layer far-field constant C_{0u} in the case $a_u = -1, p_{0u} = 1, \alpha = 2/3$. The estimates use (4.13) evaluated at $\xi = \xi_\infty$ from the numerical scheme for the IVP of section 4.1.2 in the Cartesian formulation. Sensitivity of these estimates to the initial starting value ξ_0 and the interval end point ξ_∞ are shown in both tables, where (A) takes one term initial data from (3.22) (see (4.10)) and (B) uses two terms. Convergence is illustrated for both decreasing ξ_0 and increasing ξ_∞.

	$p_0 = 1.0$				
ξ_∞	$C_{2u}^{(11)}$	$C_{2u}^{(12)}$	$C_{2u}^{(22)}$	$C_{3u}^{(12)}$	$C_{3u}^{(22)}$
10^2	-0.30990482	0.46534326	0.31572758	1.59928337	1.61329569
10^3	-0.31023872	0.05011680	-0.02166796	1.60158213	1.60317293
10^4	-0.31015132	-0.14306587	-0.17651216	1.59988952	1.59954008
10^5	-0.31011774	-0.23262842	-0.24814155	1.59855110	1.59815737
10^6	-0.31010951	-0.27415770	-0.28135224	1.59786016	1.59762797
10^7	-0.31010984	-0.29342094	-0.29675971	1.59800782	1.59788959
10^8	-0.31012031	-0.30234977	-0.30390409	1.60301904	1.60296223

Table 2: Illustration of consistent estimates of C_{2u} and C_{3u} using (4.14) and (4.15) evaluated at $\xi = \xi_\infty = 10^6$. Parameter values of the IVP in the Cartesian formulation were $a_u = -1, p_{0u} = 1, \alpha = 2/3$ with $x_0 = 10^{-6}$ and one term initial data (4.10). Each of the columns illustrate convergence with increasing ξ_∞, whilst the three estimates of C_{2u} and two of C_{3u} also show consistency.

	$a_u = -1, p_{0u} = 1$					
ξ_∞	$\tilde{\lambda}\xi^{4-2\alpha}$	$\frac{C_{1u}}{(3-\alpha)^2(C_{0u}^e)^2}$	$\tilde{\mu}\xi^{1-\alpha}$	$\tilde{\nu}\xi^{-2}$	C_{4u}^e	C_{5u}^e
10^2	2.43132790	2.43374014	-1.10105810	1.34694690	0.01802705	0.22837269
10^3	2.43586680	2.43927348	-1.10278066	1.39273518	0.01392118	0.24468657
10^4	2.43291085	2.43398342	-1.10268500	1.40459274	0.00427416	0.25399156
10^5	2.43184473	2.43211185	-1.10262794	1.40735021	0.00106151	0.25674154
10^6	2.43157052	2.43163156	-1.10261255	1.40796451	0.00024338	0.25741663
10^7	2.43150697	2.43152019	-1.10260895	1.40809886	0.00005393	0.25757071
10^8	2.43149288	2.43149540	-1.10260815	1.40812801	0.00001176	0.25760479

Table 3: Estimates of far-field constants in the case $a_u = -1, p_{0u} = 1, \alpha = 2/3$. Shown are estimates of C_{4u} and C_{5u} using (4.20) evaluated at selected ξ_∞ values. The IVP in the Cartesian stress basis formulation of section 4.1.2 is augmented with (4.16)–(4.18) for $\tilde{\lambda}, \tilde{\mu}, \tilde{\nu}$ together with two term initial data (4.19). Also recorded are the scaled values of $\tilde{\lambda}, \tilde{\mu}, \tilde{\nu}$ evaluated at ξ_∞ illustrating the far-field asymptotic behaviour (3.35)–(3.37).

$a_u = -1, \alpha = 2/3$					
	k_0 estimate	k_2 estimate	k_3 estimate	k_4 estimate	k_5 estimate
p_{0u}	$C_{0u}/p_{0u}^{\frac{2}{3}}$	$C_{2u}p_{0u}^{\frac{1}{3}}$	$C_{3u}p_{0u}^{\frac{1}{2}}$	$C_{4u}p_{0u}^{\frac{2}{3}}$	$C_{5u}p_{0u}^{\frac{4}{3}}$
1	-0.38867743	-0.31010950	1.59785794	0.00024338	0.25741663
10	-0.54676677	-2.25252646	1.23283172	0.00061235	0.16956405
10^2	-0.59134562	-2.45215759	0.51221052	0.00028688	0.15666688
10^3	-0.59804488	-2.47273913	0.26540973	0.00013285	0.15507766
10^4	-0.59881970	-2.47482551	0.18527695	0.00006165	0.15492584
10^5	-0.59890358	-2.47503272	0.15880511	0.00002861	0.15492125
10^6	-0.59891343	-2.47505394	0.15049266	0.00001328	0.15492597
10^7	-0.59891504	-2.47506181	0.15337068	0.00000616	0.15492886
10^8	-0.59891550	-2.47507794	0.17543868	0.00000286	0.15493027
10^9	-0.59891571	-2.47511203	0.24911158	0.00000133	0.15493093
10^{10}	-0.59891587	-2.47518431	0.47829641	0.00000062	0.15493123

Table 4: Illustration of convergence to the behaviours (4.7) in the case $a_u = -1, \alpha = 2/3$. The IVP numerical scheme used $\xi_0 = 10^{-6}$ with one term initial data and estimates of the far-field constants evaluated at $\xi_\infty = 10^6$. The expressions $C_{0u}^e, C_{2u}^{(11)}, C_{3u}^{(11)}, C_{4u}^e, C_{5u}^e$ were used to estimate the corresponding constants $C_{0u}, C_{2u}, C_{3u}, C_{4u}, C_{5u}$.